Advances in Colloid and Interface Science 320 (2023) 102962

Contents lists available at ScienceDirect

Advances in Colloid and Interface Science

journal homepage: www.elsevier.com/locate/cis

Historical Perspective

Zeta potential of crude oil in aqueous solution

Harry Collini [a,b], Matthew D. Jackson [a,*]

[a] Novel Reservoir Modelling and Simulation Group, Department of Earth Science and Engineering, Imperial College London, UK
[b] Now at BP International Centre for Business and Technology, Sunbury-on-Thames, Middlesex, UK

ARTICLE INFO

Keywords:
Zeta potential
Surface charge
Crude oil emulsions
Crude oil wetting layers
Potential determining ions

ABSTRACT

Despite the broad range of interest and applications, controls on the surface charge of crude oil in aqueous solution remain poorly understood. The primary data source to understand the surface charge on crude oil comprises measurements of zeta potential on individual drops or emulsions obtained using the electrophoretic method (EPM). Here we (i) collate and review previous measurements of zeta potential on crude oil, (ii) compare and contrast the results, and (iii) report new measurements of zeta potential on crude oil wetting films and layers relevant to oil-saturated porous media, obtained using the streaming potential method (SPM).

Results show that the zeta potential depends on electrolyte pH and the concentration of divalent ions Ca^{2+} and Mg^{2+}. Lower pH and higher concentration of these divalent ions yields more positive zeta potential. The isoelectric point (IEP) in simple NaCl electrolytes lies in the pH range 3–5. The IEP in simple $CaCl_2$ and $MgCl_2$ electrolytes can be expressed as pCa or pMg, respectively, and lies in the range 0–1. Close to the IEP, the zeta potential varies linearly with pH, pCa or pMg, suggesting simple Nernstian behaviour of the crude oil surface. The sensitivity of the zeta potential to pH, pCa and pMg decreases with increasing total ionic strength. The impact of pH, pCa and pMg on zeta potential varies significantly across different crude oils and differs from non-polar hydrocarbons. The potential for other multivalent ions to modify crude oil zeta potential has not been tested. Data for crude oil wetting films and layers, obtained using the SPM and strongly oil-wet porous substrates in which the solid surfaces are coated with the crude oil of interest, are comparable to those obtained using emulsions and the EPM, suggesting that the controls on zeta potential on crude oil are the same irrespective of whether the oil forms droplets or wetting layers.

The literature data reviewed here, along with new measured data, provide important insight into the effect of pH, and the concentration of divalent ions, on the zeta potential of crude oil in aqueous solution. They demonstrate relationships between ion concentration and zeta potential that are observed irrespective of crude oil composition. They also show that the crude oil composition plays a role, yet no consistent trends are observed between zeta potential and commonly measured bulk oil properties, possibly because bulk properties do not reflect the concentrations of interfacially active species in crude oil that may impact the development of surface charge. Moreover, data are extremely scarce for complex, high ionic strength electrolytes or at elevated temperature. The data reviewed and reported here have broad relevance to many engineering and industrial activities involving crude oil.

1. Introduction

Crude oil is present in many surface and subsurface settings because of natural processes or human activity [8]. The term ‘crude oil’ describes fluids containing a wide range of organic species dissolved, or in suspension, in a wide range of organic solvents. Such species primarily comprise hydrocarbons, asphaltenes, resins, paraffins, sulfuric species and ash/residue [81]. The properties of the crude oil surface, and the interface between crude oil and aqueous solution, play an important role in many engineering and industrial activities involving crude oil, including the stability of oil-in-water emulsions during transportation, storage, and separation [45,93,96], the removal of crude oil during remediation of contaminated rocks and soils [56], recovery from subsurface reservoirs [24,49,63,74], and storage of CO_2 in these reservoirs [2,57].

The focus of this paper is the zeta potential of the crude oil interface

* Corresponding author.
E-mail address: m.d.jackson@imperial.ac.uk (M.D. Jackson).

https://doi.org/10.1016/j.cis.2023.102962
Received in revised form 7 July 2023;
Available online 18 July 2023

in aqueous solution. The crude oil may be in an emulsion, or in wetting layers or films on solid surfaces. The zeta potential is a key measure of the electrical potential at the interface, and the magnitude and polarity of the zeta potential control electrostatic interactions with other charged interfaces and polar species in aqueous solution [46]. Previous studies of the crude oil interface have reported measurements of zeta potential, obtained using emulsions or droplets of crude oil in the aqueous solution of interest and the electrophoretic method (EPM) [29,55,62–64,68,85,86]. Zeta potential measurements on individual droplets or emulsions comprise the primary data source to characterise the electrical charge on crude oil in aqueous solution. Measurements of zeta potential on crude oil wetting layers or films in contact with aqueous electrolytes have not been reported.

The aims of the paper are threefold: (1) to collate and review previous measurements of the zeta potential of crude oil in aqueous solution as a resource for future studies, (2) to compare and contrast the results of these studies to determine key controls on zeta potential and where uncertainties remain, and (3) to report new measurements of zeta potential on solid surfaces wetted by crude oil in aqueous solution, testing a parameter space that has not been investigated previously. There has been no comprehensive review of zeta potential measurements on crude oil to date, although some studies have collated data to calibrate and test models for the development of electrical charge on the crude oil surface (e.g. [13,15,87]).

The paper focuses primarily on experimental data, but we draw on published models to understand and contextualise the data in terms of the key controls on the magnitude and polarity of the zeta potential measured on crude oil. We also contrast the data with that obtained using pure, non-polar hydrocarbon liquids, which display a pH-dependent zeta potential that has been interpreted to be caused by specific adsorption of the hydroxide ion (e.g. [10,11,25,26,66,82]) although other mechanisms have also been proposed [76,88]. The pH-dependence of the zeta potential on non-polar liquid hydrocarbons has been shown to be largely independent of hydrocarbon type. As we show here, crude oils display far more variability in the pH-dependence of the zeta potential, with different crude oils showing different behaviour; these data suggest that the mechanisms causing development of surface charge are different, or there are additional mechanisms, compared to non-polar oils (e.g. [13,15,21,33,84,87]). A key difference between crude oils and pure hydrocarbons is the presence of species such as asphaltenes and resins in crude oils which are known to be interfacially active: their type and concentration control interfacial properties such as surface tension and wetting (e.g. [94–96]).

We report new data measured on solid surfaces wetted by the crude oil of interest and an experimental methodology based on the streaming potential method (SPM). We explore a range of crude oils in contact with aqueous solutions; we also investigate the impact of the Ca^{2+} ion on the zeta potential because the limited experimental data reported to date [62,68,74] suggest the presence and concentration of the Ca^{2+} ion has a significant impact on the zeta potential of crude oil in aqueous solution. The literature data reviewed here, along with our new measured data, provide important insight into the effect of pH, and the concentration of key ions such as Ca^{2+} and Mg^{2+}, on the zeta potential of crude oil in aqueous solution, demonstrating relationships between ion concentration and zeta potential that are observed irrespective of crude oil composition. They suggest that crude oil composition plays a role, although no consistent trends are observed between zeta potential and commonly reported bulk oil properties.

2. Zeta potential and the electrical double layer

The theory of the electrical double layer and the concept of the zeta potential have been described in numerous textbooks and journal articles (e.g. [3,46,75,92]). We provide here only a brief overview of the key elements relevant to the methods used to obtain the zeta potential data reported here.

2.1. The electrical double layer

When an immiscible or sparsely miscible fluid such as crude oil, is placed in contact with an aqueous electrolyte, an electrical charge develops on the interface between the two phases which creates a region of equal and opposite charge in the adjacent electrolyte in an arrangement often termed the electrical double layer (EDL). Counter-ions in the electrolyte with an opposing polarity are attracted to the interface, which locally increases their concentration; conversely, co-ions with the same charge are repelled. The counter-ions screen the surface electrical charge, so the magnitude of the electrical potential in the electrolyte decreases with distance from the interface, falling to zero some distance away (typically of order nm) in the neutral bulk electrolyte (e.g. [46]; Fig. 1). If the fluid contains polar species, an EDL may also develop in the fluid on the opposite side of the interface from the electrolyte.

Crude oil can wet solid surfaces in the presence of an aqueous electrolyte, in which case a film or layer of oil separates the solid from the electrolyte and the properties of the crude oil dominate the interfacial behaviour [8,16–18,23,44]. Wetting films are typically of nanometre thickness; wetting layers are present in porous materials and are typically of micrometre thickness, controlled by capillary forces and pore geometry (e.g. [61]). Fig. 1 shows a schematic of the EDL for (a) a non-polar hydrocarbon droplet in an aqueous electrolyte in which surface charge results from adsorption of hydroxide ions (e.g. [82]); (b) a crude oil droplet in an aqueous electrolyte in which surface charge results from adsorption of hydroxide ions and polarisation of surface active sites (e.g [13]) and (c) a crude oil film that coats (wets) a solid surface in contact with the same electrolyte (adapted from [24]). In all cases, we assume the oil develops a negative surface charge.

The Gouy-Chapman-Stern (GCS) model extends the classical EDL model, subdividing the excess charge in the electrolyte into a ‘Stern layer’ and a ‘diffuse layer’ ([46]; Fig. 1). The Stern layer contains ions that are immobile relative to the surface, because they are adsorbed or attached. Typically, the excess counter-charge in the Stern layer is insufficient to balance the excess surface charge, leading to the accumulation of excess counter-charge in the diffuse layer. The electrical potential decreases through the diffuse layer until it reaches zero in the neutral electrolyte [46]. The zeta potential is defined as the electrical potential at a notional ‘shear’ plane. It is assumed that ions in the diffuse layer are mobile beyond the shear plane, which lies some distance away from the surface (Fig. 1). The shear plane is often assumed to coincide with the Stern plane or treated as a variable which can be adjusted in models to match experimental data (e.g. [13,37,75]).

2.2. Electrokinetic phenomena and measurement of the zeta potential

The surface charge of most solid interfaces in aqueous solution can be measured by potentiometric titration (e.g. [22]). Solid particles are placed in an acid or base electrolyte and allowed to equilibrate before being neutralised. The surface charge is calculated from the amount of acid/base required to neutralise the sample. However, potentiometric titration of a fluid such as oil in aqueous solution measures the total charge present in the bulk fluid, rather than at the fluid-fluid interface (e.g. [30]). Potentiometric titration of crude oil measures the total concentrations of negatively and positively charged species such as hydrocarbons and asphaltenes [83]. These bulk concentrations are commonly termed the acid number (AN) and the base number (BN) respectively. Since the surface charge cannot be determined directly, zeta potential measurements are the primary source of data available to understand the electrical properties of the crude oil interface (e.g. Fig. 2).

Tangential motion of mobile excess charge along the shear plane leads to electrokinetic phenomena. Experimental methods to measure the zeta potential make use of these electrokinetic phenomena. The zeta potential data reported here were measured, with one exception, using either (i) the EPM, in which charged particles or droplets are mobilised

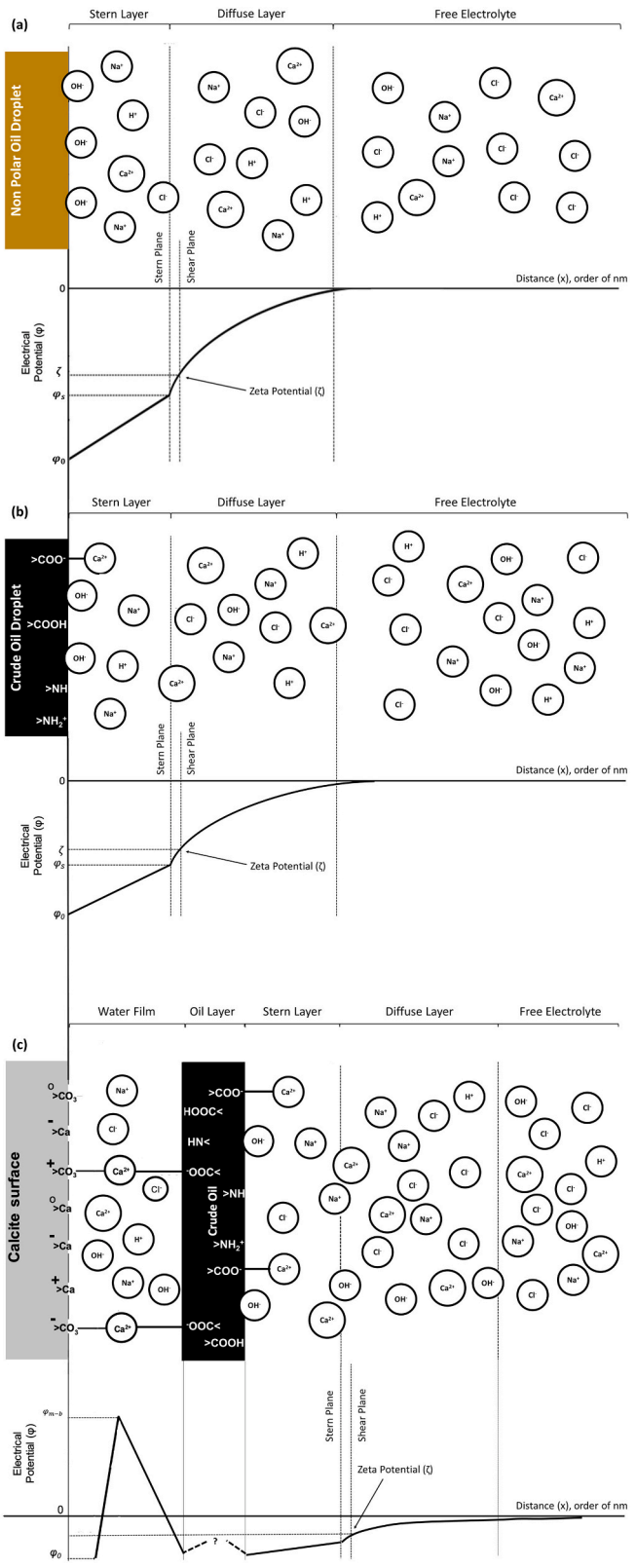

Fig. 1. Schematic of a double layer model for (a) a non-polar hydrocarbon droplet in an aqueous electrolyte in which surface charge results from adsorption of hydroxide ions (e.g. [82]); (b) a crude oil droplet in an aqueous electrolyte in which surface charge results from adsorption of hydroxide ions and polarisation of surface active sites, and (c) a crude oil film (a few nanometeres thick) that coats (wets) a solid surface in contact with the same electrolyte (adapted from [24]). In this case, the solid surface is calcite. The oil is assumed to have a negative surface charge.

relative to a stationary electrolyte by application of an electrical potential field, or (ii) the streaming potential method (SPM), in which an electrical potential difference is created by flowing an electrolyte relative to a stationary solid by application of a fluid pressure gradient [29,46].

2.2.1. Electrophoretic methods

The EPM is typically implemented in commercially available equipment such as a zetasizer (e.g. [29]). An electrical potential field is applied to a suspension of powdered or crushed solid particles, or to an emulsion of fluid droplets, in the electrolyte of interest. The electrical potential causes the particles or droplets to move, and their velocity is measured. The magnitude of the velocity is normalized by the magnitude of the electric field to yield the electrophoretic mobility.

To interpret zeta potential from measured electrophoretic mobility requires a model for the distribution of charge on, around and possibly within the particles or droplets [29,39,52,71]. In some of the studies reviewed here, the model used to calculate the zeta potential was not reported [62,64,68,74,85,86]. The remaining studies all use models that assume hard (impermeable) colloidal particles with a homogeneous distribution of charge on their surface, no slip of the electrolyte at the surface (corresponding here to the shear plane; Fig. 1), negligible excess (surface) electrical conductivity (i.e. Duhkin number $Du << 1$) and no polarisation within the electrical double layer [29,39,71].

In some studies, the zeta potential was calculated using the Gouy-Chapman (GC) model for the distribution of electrical charge in the diffuse layer [18,21,32]; in most, the zeta potential was calculated assuming the ratio of the particle size to the EDL thickness is large ($a/\lambda >> 1$, where λ is the Debye length and a is the particle or droplet size; i.e. there is a thin EDL) in which case the GC model can be linearized to yield the classical Helmholtz-Smoluchowski equation [46]

$$u_e = \frac{\varepsilon\zeta}{\mu} \tag{2.1}$$

where ζ is the zeta potential, ε is the permittivity (F m^{-1}) and μ is the viscosity of the electrolyte (Pa s) [5,33,55,66,67,82,87]. Beattie and Djerdjev [10] used the electroacoustic method but provided no details on the measurements obtained or the model used to calculate the zeta potential.

The crude oil or hydrocarbon droplets in the EPM experiments reported here are typically of order microns in size while the EDL thickness for the electrolytes tested is of order nanometers, consistent with the thin EDL assumption ($a/\lambda >> 1$; in the studies reported here, $a/\lambda > 20$ is estimated from the data available). The conditions for which surface electrical conductivity and EDL polarisation may be important have been determined previously (e.g. [29]). The condition $Du << 1$ is achieved when $a/\lambda >> 1$ and for smaller values of zeta potential and a larger proportion of charge beyond the shear plane; it is estimated (from limited data) to be met in the studies reported here, except perhaps for higher values of zeta potential (> 80 mV) which typically correspond to higher pH and/or more dilute electrolytes.

The sparse solubility of crude oil and hydrocarbons in aqueous solution inhibits the transfer of charge across the interface, consistent with the assumption of hard particles (note that the term 'hard' does not refer to the mechanical rigidity of the particles but to their ion and hydrodynamic permeation; [39]). However, momentum transfer may occur causing flow within the fluid droplet, in which case a shear plane (Fig. 1a) cannot be defined. Momentum transfer is reduced if the fluid within the droplet has high viscosity and/or if there is a layer of adsorbed surface-active components (e.g. [29,70]). Decane droplets in aqueous solution have been shown to approximate hard particle electrokinetic behaviour [70]. The hydrodynamic problem is further complicated by the observation of slip at hydrophobic surfaces (e.g. [38,52,53]). A slip length, typically of order of a few nanometers, has been identified at such surfaces, although slip on hydrophobic fluid

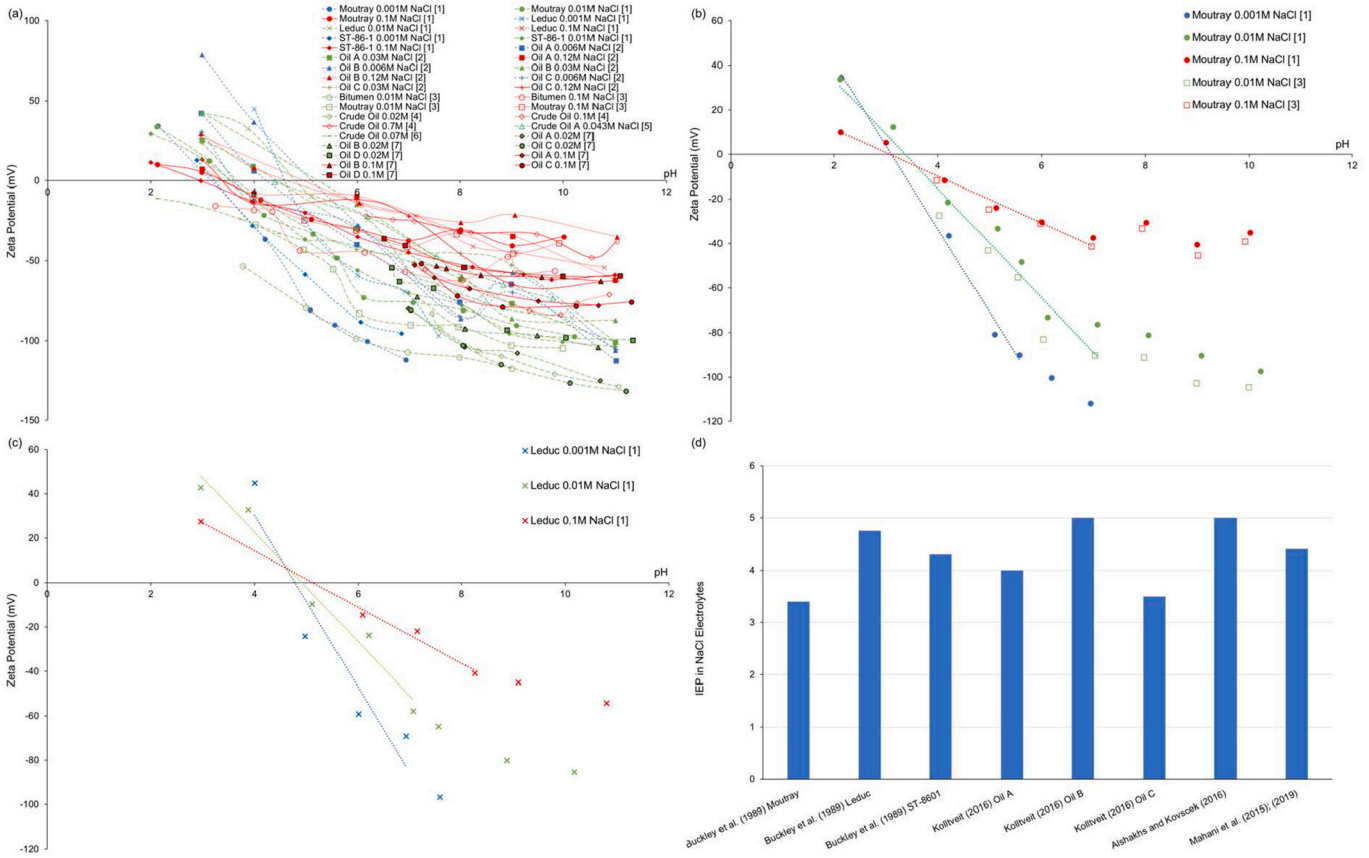

Fig. 2. Published zeta potential data for crude oil emulsions in NaCl electrolytes measured using the EPM. Plot (a) shows all data plotted against pH: blue lines represent measurements obtained in the ionic strength range 10–3 $< I \leq$ 0.01 M; green lines in the range 0.01 $< I \leq$ 0.1 M and red lines at $I >$ 0.1 M. Data from [1] Buckley et al. [18] [2] Kolltveit [55] [3] Chow and Takamura [21] [4] Takeya et al. [85] [5] Mahani et al. [64] [6] Farooq et al. [33] [7] Takeya et al. [86]. Plots (b) and (c) show data for specific crude oils and dashed lines denote linear fit to the data. Plot (d) shows the IEP for the different crude oils tested, interpreted from the data shown in (a). See Table 1 for the electrolytes, crude oils, experimental conditions, and experimental method. (For interpretation of the references to colour in this figure legend, the reader is referred to the web version of this article.)

droplets has not yet been investigated. Despite its ubiquity in published studies, the assumption that hydrocarbon and crude oil droplets can be treated as hard particles with no slip is a significant simplification that requires further investigation, as do the conditions for applicability of Eq. (2.1). Here we collate zeta potential data as reported in the literature.

2.2.2. Streaming potential method

The SPM requires equipment to impose a pressure difference (ΔP) that causes the electrolyte of interest to flow through a capillary, porous medium or packed bed, or along a flat surface or membrane, of the solid material of interest [29,46]. The pressure gradient causes flow of excess charge in the diffuse layer relative to the charged surface, giving rise to an electrical potential difference across the sample (ΔV) which is measured [29,46]. The potential difference is normalized by the pressure difference to yield the streaming potential coupling coefficient (C), which is typically treated as an isotropic quantity. Here we use a porous medium in which the solid surfaces are coated by the crude oil of interest. Assuming a hard crude-oil interface, negligible electrical surface conductivity and that the ratio of the pore size to the EDL thickness is large ($r/\lambda >> 1$, where r is the pore size; i.e. there is a thin EDL) the zeta potential can be related to the coupling coefficient by the Helmholtz-Smoluchowski equation

$$C = \frac{\Delta V}{\Delta P} = \frac{\varepsilon \zeta}{\sigma_e \mu} \tag{2.2}$$

where σ_e is the electrolyte electrical conductivity (S•m^{-1}). The zeta potential obtained is an average across all solid-fluid interfaces in the sample. If surface electrical conductivity is significant, its contribution can be corrected for using a modified form of Eq. (2.2) [60]

$$C = \frac{\Delta V}{\Delta P} = \frac{\varepsilon \zeta}{\sigma_m \mu F} \tag{2.3}$$

where σ_m represents the conductivity of the medium (S•m^{-1}) when saturated with the electrolyte of interest and F is the formation factor of the medium, defined as the ratio of the electrolyte conductivity, σ_e, to the medium conductivity, σ_m, when surface electrical conductivity is negligible. In the experiments reported here, we assume the crude oil is impermeable to charge and there is no flow within crude-oil wetting films and layers, so the crude-oil interface is hard. We note that slip has been observed during flow past hydrophobic surfaces (e.g. [52]) but, consistent with the EPM studies reviewed here, we do not attempt to account for slip when calculating the zeta potential.

3. EPM measurements of zeta potential on crude-oil droplets and emulsions in aqueous solution

3.1. Electrolyte concentration and composition

3.1.1. Effect of pH

Much of the published zeta potential data obtained on emulsions of crude oil droplets in aqueous electrolytes have explored the effect of pH in simple NaCl electrolytes. Fig. 2a collates zeta potential measurements obtained using such electrolytes as a function of pH. Inconsistencies in

the experimental conditions across different studies (see Table 1) mean these data are not always directly comparable, so we group by orders of magnitude of ionic strength. Data regarding the properties of the crude oils can be found in Table 1. Note that no studies reported error bars with their experimental data.

The zeta potential is consistently negative at high pH and becomes increasingly positive with decreasing pH. The zeta potential changes polarity at the isoelectric point (IEP), defined as the pH at which the zeta potential is zero. At pH values close to the IEP, the relationship between zeta potential and pH is approximately linear (e.g. Fig. 2b, c). The gradient of the linear relationship increases with decreasing ionic strength, varying over the range − 10 mV/decade at 0.1 M ionic strength, to −40 mV/decade at 10^{-3} M ionic strength (Table 3). At higher pH, the sensitivity of the zeta potential to pH decreases.

There is a large variation in the magnitude of the zeta potential measured on different oils for a given pH and electrolyte ionic strength, and the range is typically larger at low ionic strength and high pH (e.g. Fig. 2a). Furthermore, the IEP varies across the range pH 3–5 for different datasets, including different crude oils and electrolyte ionic strength (Fig. 2d). In the more dilute (10^{-3} - 0.01 M) electrolytes, close to the average IEP of ca. pH 4, the range of measured zeta potential reaches almost 100 mV and includes both positive and negative values (Fig. 2a). This variation may be due to differences in experimental procedure (Table 1) or could reflect the wide range of surface charge on different crude oils. Mechanisms that may control the pH dependence of the zeta potential of crude oil are discussed later in the paper.

For comparison, we show measured zeta potential from pure, non-polar hydrocarbons in simple NaCl electrolytes as a function of pH (Fig. 3); again, no studies reported error bars. Compared to the crude oils, the spread of values for a given value of pH is small, especially for pH > 6; moreover, only negative zeta potentials are observed, so an IEP cannot be defined. We note that Creux et al. [25] observed positive zeta potential for octane, decane and dodecane in aqueous solution, with the IEP in the range pH = 2 to pH = 3. However, no NaCl was added to their pure water electrolyte, so their data cannot be directly compared to those shown in Fig. 3. For pH < 6, the relationship between zeta potential and pH for the non-polar hydrocarbons is approximately linear and independent of hydrocarbon type (Fig. 3). The gradient of the linear relationship is −19 mV/decade (Table 3).

A linear relationship is consistent with Nernstian behaviour of a charged interface and suggests the electrical double layer can be described by the simple GCS model close to the IEP (e.g. [46]). In the GCS model, the gradient of the zeta potential can be described by (e.g. [34]):

$$\left.\frac{d\zeta}{dpPDI}\right|_{\zeta\to 0} = \frac{-2.303\frac{k_B T}{ze}}{\left(1+\frac{C_d}{C_s}\right)exp(\kappa\delta)} \tag{3.1}$$

where k is the Boltzmann constant, T the absolute temperature, z the valence of the potential determining ion (PDI), pPDI denotes the negative logarithm of the PDI concentration in M, e the elementary charge on an electron, κ the inverse Debye length ($1/\lambda$), C_d and C_s are the capacitance per unit area of the diffuse and Stern layers respectively and δ the distance of the shear plane from the Stern plane. The Stern layer capacitance for a given oil can therefore be calculated from the gradient of the linear regression (Table 3) and Eq. (3.1). The diffuse layer capacitance is assumed to be approximated by $\kappa\varepsilon$ where ε is the electrolyte permittivity [4]. The simplest assumption that the Stern plane coincides with the shear plane is employed, so we set $\delta = 0$ (Fig. 1). The Stern layer capacitance, C_s, calculated in this way is reported in Table 3. Despite the large range in gradients for different ionic strength electrolytes, the Stern layer capacitance for the crude oils remains approximately constant, varying by <25% around the mean value of 0.16 F•m^{-2}. For comparison, the Stern layer capacitance for the non-polar hydrocarbons is much lower at 0.04 F•m^{-2} (Table 3).

3.1.2. Effect of divalent cations

The impact of divalent cations Ca^{2+} and Mg^{2+} on the zeta potential of crude oil in aqueous emulsions has been studied by several authors (Fig. 4a), although the data are considerably less abundant than for pH (compare Figs. 2a and 4a). Note again that no studies reported error bars with their experimental data. The zeta potential typically shows a linear variation with divalent ion concentration for a given crude oil and electrolyte, where concentration is expressed as pCa or pMg (or more generally, pPDI). The zeta potential is negative in the low concentration range (pPDI >1) but charge inversion is observed for some crude oils at higher concentration (pPDI <0.5) with the IEP in the range pPDI = 0 to 1, depending on pH. The sensitivity (gradient) of the zeta potential to pPDI increases with increasing pH over the range 4–10 (e.g. Fig. 4b) but becomes relatively insensitive at high pH (e.g. Fig. 4c).

Comparison of these data for crude oil with data for non-polar hydrocarbons is challenging because measurements of zeta potential on non-polar hydrocarbons in aqueous electrolytes containing divalent ions are few. Only Dunstan and Saville [32] systematically tested the effect of varying divalent ion concentration, using solid docosane particles in $CaCl_2$ electrolyte (Fig. 5). No error bars were reported. The zeta potential shows a linear variation with pCa, becoming less negative with decreasing pCa, but the IEP cannot be identified because there is no charge inversion.

The linear relationship between zeta potential and pPDI observed for crude oil and docosane is again consistent with Nernstian behaviour of the charged interface. Applying the GCS model (Eq. (3.1)) allows calculation of the Stern layer capacitance (Table 3). The Stern layer capacitance for the crude oils in contact with Ca^{2+} varies by a factor of 6 and reaches a maximum value of 5.63 F•m^{-2}, in contrast to the smaller values and variation observed in response to pH change (Table 3). Higher capacitance is observed at higher pH for the crude oils. In comparison, the capacitance for docosane in contact with Ca^{2+} is 0.78 F•m^{-2}, comparable to the smallest value obtained for the crude oil, and much larger than the values obtained for non-polar oils as a function of pH (Table 3).

The available data suggest that the zeta potential on crude oil is more sensitive to changes in Ca^{2+} compared to Mg^{2+}, noting that Takeya et al. [85,86] obtained a steeper gradient for zeta potential versus pCa (Fig. 4d); moreover, Nasralla and Nasr-El-Din [68] reported a positive zeta potential at pCa = 0.34 and pH = 4, but a negative zeta potential for the same oil at pMg = 0.28 and pH = 4. The potential for other multivalent ions to act as PDIs for the crude oil surface has not been tested, although such ions are often present in natural brines and engineered electrolytes (e.g. Table 2). For comparison, Dunstan and Saville [32] observed a non-monotonic variation in zeta potential on docosane particles with $AlCl_3$ concentration (Fig. 5), recording positive zeta potential over most of the concentration range with a maximum in the range 2 < pPDI <4.

3.1.3. Monovalent ions and total ionic strength

The magnitude of the zeta potential on crude oil generally decreases with increasing ionic strength in NaCl electrolytes (Fig. 2), as predicted for indifferent ions by simple models of the diffuse layer (e.g. [46]). Monovalent ions such as Na, K, Cl are typically assumed to be indifferent to most interfaces in aqueous solution: they show no tendency to adsorb onto the surface. However, data relating zeta potential and Na^+ concentration for a given pH and crude oil concentration are sparse (e.g. Fig. 6a). These data show that the sensitivity does vary for different crude oils; however, the IEP (expressed as pH) is independent of Na concentration (Fig. 6b) and increasing Na^+ concentration does not yield charge inversion, in contrast to the divalent ions. Again, no studies reported error bars and it is not clear whether the small variations in sensitivity arise from experimental errors. Marinova et al. [66] observed a decrease in the magnitude of the zeta potential on xylene with increasing NaCl concentration and interpreted this to represent the decrease in diffuse layer thickness with increasing ionic strength.

Table 1
Summary of studies reporting experimental zeta potential data obtained on crude oil emulsions in aqueous electrolytes. The compositions of the complex electrolytes are given in Table 2. All reported crude oil compositional data are shown.

Reference	Method	Material	Name	Density at 25 °C (kg/m^3)	Viscosity at 25 °C (mPa.s)	AN (mgKOH/g)	BN (mgKOH/g)	AN/BN Ratio	Asphaltene content (wt%)	Electrolyte compositions	Ionic strength (M)	Temperature (°C)	IEP in NaCl electrolytes (pH)
Buckley et al. [18]	EPM	Crude Oil	Moutray	838	5.23	0.26	2.52	0.10	N/A	NaCl	10^{-3} - 0.1	25	3.4
			Leduc	913	2.49	0.15	0	N/A	N/A				4.75
			ST-86-1	875	13.01	0.15	8.14	0.02	N/A				4.3
Kolltveit [55]	EPM	Crude Oil	A	904	36	3.01	N/A	N/A	0.25	NaCl; NaCl + $CaCl_2$	0.006–0.12	25	4
			B	934	277	2	N/A	N/A	2.04				5
			C	891	22	0.98	N/A	N/A	0.39				3.5
Chow and Takamura [21]	EPM	Crude Oil	Moutray	838	5.23	0.26	N/A	N/A	0.18	NaCl; $CaCl_2$	0.01–0.1	25	N/A
		Bitumen	Bitumen	1010	400,000	2	N/A	N/A	17				N/A
Alshakhs and Kovscek [5]	EPM	Crude Oil	Crude Oil	831	2.4	1.15	1.25	0.92	N/A	$MgSO_4$; Mg; SO_4; complex electrolytes in Table 2	10^{-4} - 0.01	25	5
Nasralla and Nasr-El-Din [68]	EPM	Crude Oil	A	886	32.2	0.18	1.65	0.11	N/A	NaCl; $CaCl_2$; $MgCl_2$	0.018–0.01	25	N/A
			B	828	20.4	0.11	0.62	0.18	N/A				N/A
Takeya et al. [85]	EPM	Crude Oil	Crude Oil	919	8.398	0.39	1.86	0.21	24.2	NaCl; $CaCl_2$; complex electrolytes in Table 2	0.002–0.8	50	N/A
Takeya et al. [86]	EPM	Crude Oil	A	0.831 (15C)	N/A	0.17	1.08	0.16	1.6	NaCl; $CaCl_2$; complex electrolytes in Table 2	0.002–4.42	25	N/A
			B	0.871 (15C)	N/A	0.11	0.78	0.14	12.3				
			C	0.895 (15C)	N/A	1.06	1.42	0.75	4.2				
			D	0.869 (15C)	N/A	0.07	0.13	0.54	2.2				
Lu et al. [62]	EPM	Crude Oil	Oil 1	952	2190	0.21	5.6	0.04	3.3	NaCl; $MgCl_2$	10^{-5} - 3	25–65	N/A
			Oil 2	888	125	0.18	1.14	0.16	2.1				N/A
Mahani et al.[64]	EPM	Crude Oil	Crude Oil	857	20.75	0.52	1	0.52	0.28	NaCl; complex electrolytes in Table 2	10^{-3} - 3.7	25	4.4
Mehraban et al. [67]	EPM	Crude Oil	Crude-A	840 (90C)	2.35 (90C)	0.14	N/A	N/A	0.2	Complex electrolytes in Table 2	0.832	28–62	N/A
			Crude-B	870 (90C)	3.3 (90C)	0.1	N/A	N/A	6				N/A
Tetteh et al. [87]	EPM	Crude Oil	LKC Crude Oil	840 (40C)	5.86 (40C)	0.17	0.11	1.55	0.73	NaCl; KCl; $CaCl_2$; $MgCl_2$; Na_2SO_4; complex electrolytes in Table 2	0.04–3.27	25–40	N/A
Pooryousefy et al. [74]	EPM	Crude Oil	Texas Crude	890	N/A	1.58	1.02	1.55	N/A	$CaCl_2$	0.018–0.45	25	N/A
Farooq et al. [33]	EPM	Crude Oil	Crude Oil	880	11.1	2.7	0.8	3.38	0.7	NaCl; $CaCl_2$	0.065	25	N/A

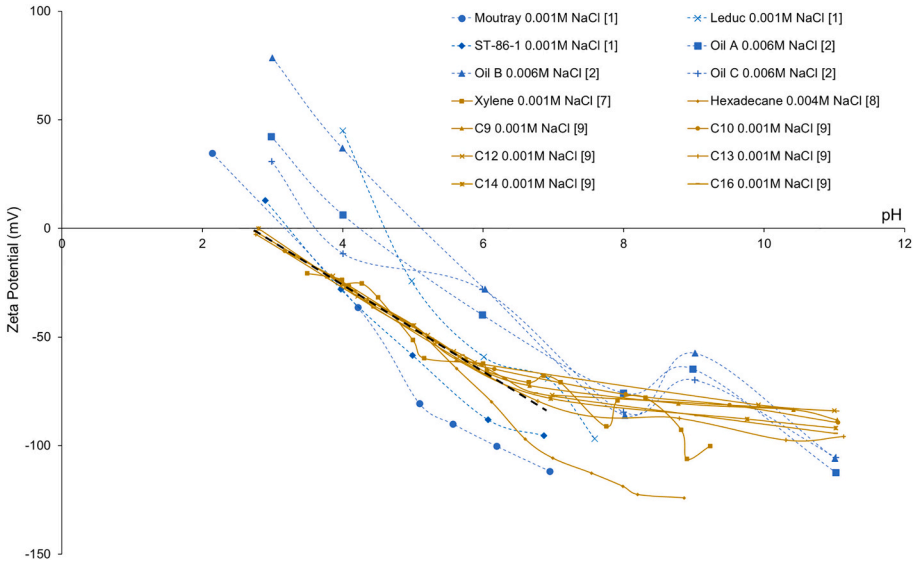

Fig. 3. Published zeta potential data for emulsions of non-polar hydrocarbons in NaCl electrolytes measured using the EPM, plotted with crude oil data extracted from Fig. 2 for the comparable range of NaCl ionic strength ($10–3 < I \leq 0.01$ M). Data from [1] Buckley et al. [18] and [2] Kolltveit [55] as in Fig. 2. Data from [7] Marinova et al. [66] [8] Beattie and Djerdjev [10] [9] Stachurski and Michalek [82]. Dashed black line denotes linear fit to the data for non-polar hydrocarbons for pH < 6.

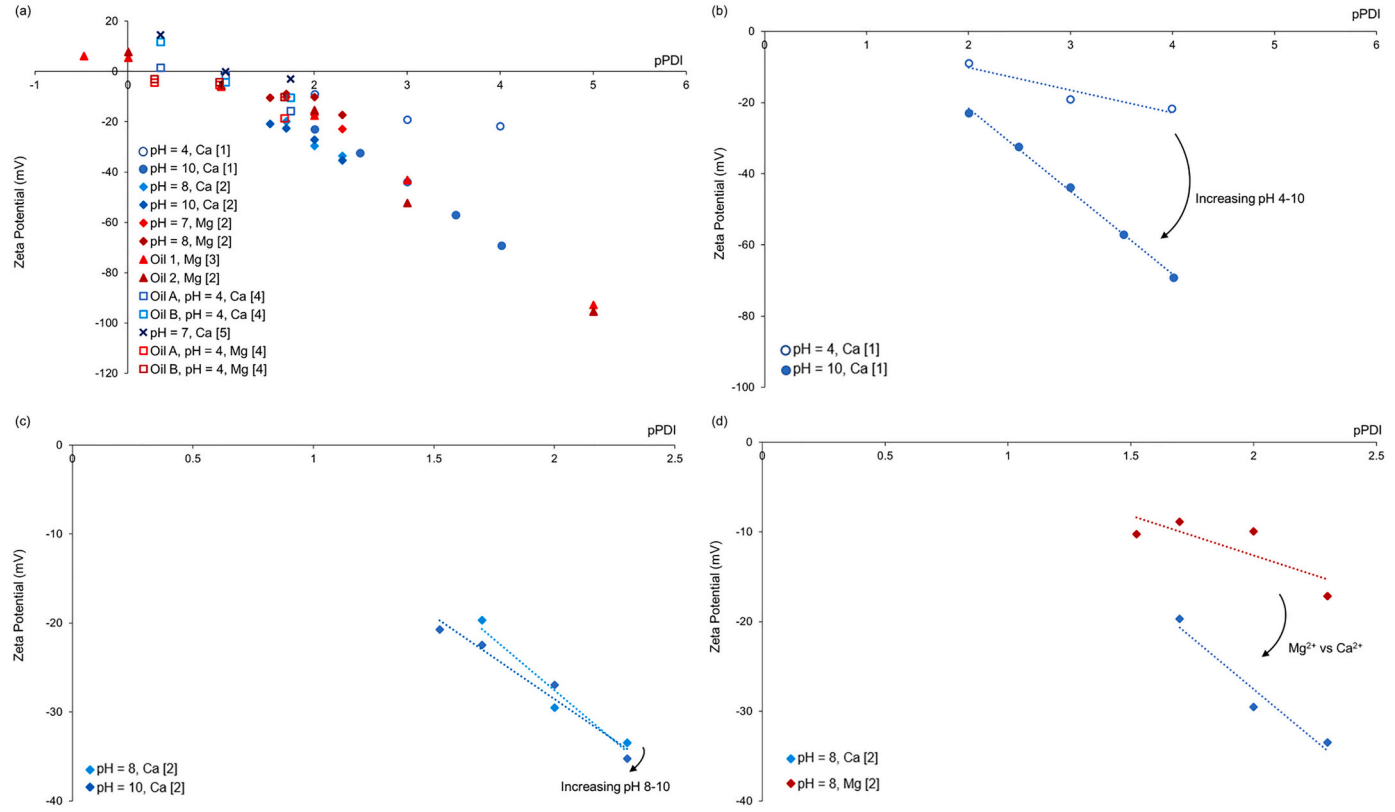

Fig. 4. Published zeta potential data for emulsions of crude oil in CaCl2 and MgCl2 electrolytes. Plot (a) shows all data plotted against pPDI (where PDI denotes Ca or Mg and p denotes the negative logarithm of the concentration in M): blue datapoints show data plotted against pCa; red datapoints show data plotted against pMg; open symbols denote data acquired at low pH (pH = 4); closed symbols denote data acquired at neutral to high pH (7–10); symbol shapes denote different studies. Plots (b), (c) and (d) show selected data, demonstrating the impact of (b) and (c) pH on the sensitivity of the zeta potential to pCa; (d) difference in sensitivity between Ca^{2+} and Mg^{2+}. Dashed lines denote linear fit to the data. See Table 1 for the electrolytes, crude oils, experimental conditions and experimental method. Data from [1] Chow et al. [18] [2] Takeya et al. [85] [3] Lu et al. [62] [4] Nasralla and Nasr-El-Din [68] [5] Pooryousefy et al. [74] [6] Takeya et al. [86]. (For interpretation of the references to colour in this figure legend, the reader is referred to the web version of this article.)

3.1.4. Complex electrolytes

Only a few studies have measured the zeta potential of crude oils in complex, high ionic strength electrolytes and at elevated temperature, yet these conditions are relevant to many engineering systems and subsurface reservoirs. Fig. 7 collates published zeta potential measurements on crude oil in complex, multi-ion electrolytes representative of natural subsurface brines. The experiments are summarized in Table 1 and the electrolyte compositions are reported in Table 2. Fig. 7a shows how the zeta potential varies as a function of pH in such electrolytes whilst Fig. 7b shows data where the pH was not reported. No

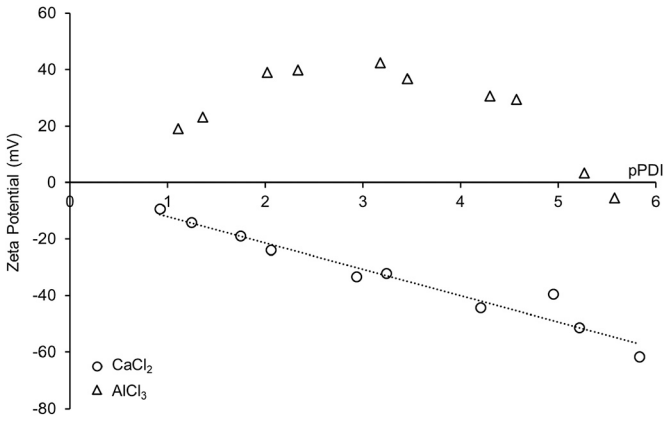

Fig. 5. Published zeta potential data for solid docosane particles in $CaCl_2$ and AlCl*3* electrolytes [32] as a function of pPDI where PDI denotes Ca^{2+} or Al^{3+}. Electrolyte pH was not reported. Dashed line denotes linear fit to the data.

studies reported experimental errors. There are no comparable studies for non-polar oils.

Many of the same trends observed in Figs. 2 and 4 are also observed in Fig. 7. The zeta potential is positive at low pH and becomes increasingly negative with increasing pH (Fig. 7a) with an IEP around pH = 4. However, the impact of varying pH decreases with increasing ionic strength. The zeta potential increases in magnitude with decreasing electrolyte ionic strength (increasing dilution) (Fig. 7b). This increase is consistent with double layer expansion and the reduction in the concentration of PDIs (Table 2). However, the data are sparse and the impact of high ionic strength electrolytes on the zeta potential of the crude oil surface remains a key area for future study.

3.2. Effect of temperature

Only three studies have examined the impact of temperature on the zeta potential of crude oil ([62,67,87]; Table 1 and Fig. 8) and the data show contrasting trends. Lu et al. [62] reported the temperature dependency of two crude oils in NaCl and $MgCl_2$ electrolytes. The zeta potential of their Oil 1 was independent of, or only weakly dependent on temperature, whereas the zeta potential of their Oil 2 decreased in magnitude with increasing temperature in dilute electrolytes (<0.01 M). In higher concentration electrolytes, the zeta potential of both oils was independent of temperature. Tetteh et al. [87] and Mehraban et al. [67] reported zeta potential measurements in complex electrolytes (see Table 2) for three different crude oils (Table 1) at 25 and 40 °C, and 28 and 60 °C, respectively. Contrary to the data from Lu et al. [62], the zeta potential increased in magnitude with increasing temperature, irrespective of electrolyte composition. Data exploring the effect of temperature on the zeta potential of crude oil in aqueous solution are too sparse and contradictory to draw firm conclusions, and there are no comparable data for non-polar oils.

3.3. Crude oil composition

Despite the broad range of crude oil compositions, few studies have explored the link between crude oil composition and zeta potential. Moreover, the scarce data available relates zeta potential to measurements of bulk AN and BN, rather than interfacial oil properties or a more detailed description of oil composition. The limited available data show no correlation between these bulk properties and zeta potential (Fig. 9), which is perhaps unsurprising given that it is not clear if, or how, bulk and surface properties are related or whether polar oil components control the development of surface charge (e.g. [33]). We discuss this issue further in a later section.

4. SPM measurements of the zeta potential on crude oil wetted solid surfaces in contact with aqueous electrolytes

4.1. Indirect estimates of zeta potential using the SPM

It has been shown that the zeta potential measured using the SPM on samples of natural porous carbonate rocks saturated with electrolyte and crude oil is affected by the wetting state. Jackson and Vinogradov [50] measured a positive zeta potential on natural, water-wet reservoir carbonates in a high ionic strength reservoir brine (FMB, Table 2) which became less positive after becoming more wetting to crude oil. The wettability of the samples was characterised using the Amott water wetting index [6]:

$$I_w = \frac{V_{WSI}}{V_{WSI} + V_{WFI}} \tag{4.2}$$

where V_{WSI} is the volume of water spontaneously imbibed (SI) into the sample and V_{WFI} is the additional volume of water that can be forced into the sample by applying a pressure gradient.

Jackson and Vinogradov [50] proposed that the zeta potential at oil-wet mineral surfaces reflects the properties of the crude oil interface rather than the mineral interface. A more negative zeta potential measured in an oil-wet sample as compared to a water-wet sample is therefore consistent with a zeta potential at the crude oil interface that is more negative than that of the mineral interfaces, and vice-versa.

Jackson et al. [51] and Collini et al. [24] extended this work and

Table 2
Ionic composition of the complex electrolytes used by various authors to represent natural brines. FMB and FW denote typical brines found in deep saline aquifers and hydrocarbon reservoirs; SW denotes seawater, dSW denotes dilute seawater and the preceding number the dilution factor, and LS denotes 'low salinity' brine.

		Concentration (mM)							
Reference	Electrolyte	Na^+	Ca^{2+}	Mg^{2+}	SO_4^{2-}	Cl^-	K^+	Sr^{2+}	HCO_3^-
	25dSW	23.3	0.50	2.70	1.40	27.2	0.50	0	0.10
Mahani et al. [64]	SW	583	12.7	66.6	35.3	680	12.4	0.20	2.90
	FW	2170	363	134	2.40	3150	0	0	2.70
Alshakhs and Kovscek [5]	100dSW	7.50	0	0.90	0.40	8.70	0	0	0
	1000dSW	0.70	0	0.10	0	0.90	0	0	0
Mehraban et al. [67]	SW	550	12.5	67.5	31.6	657	10.7	0	1.20
	FW	2090	275	115	2.70	2871	12.8	0	0
Tetteh et al. [87]	SW	417	55.0	23.0	0.50	574	2.60	0	0
	LS	25.4	3.40	1.40	0	35.0	0.20	0	0
Takeya et al. [85]	FW	529	53.3	13.2	0.80	634	3.50	0	2.30
	SW	493	11.0	44.2	27.9	534	11.3	0	2.00
Takeya et al. [86]	FW	2700	583	52.8	2.56	3600	0	0	0
	SW	604	15.0	65.0	35.6	685	0	0	0
Jackson & Vinogradov [50]	FMB	2020	351	46.7	2.50	2809	0	0	5.70
Jackson et al. [49]	FMB	1999	421	91.0	2.00	3020	0	0	0

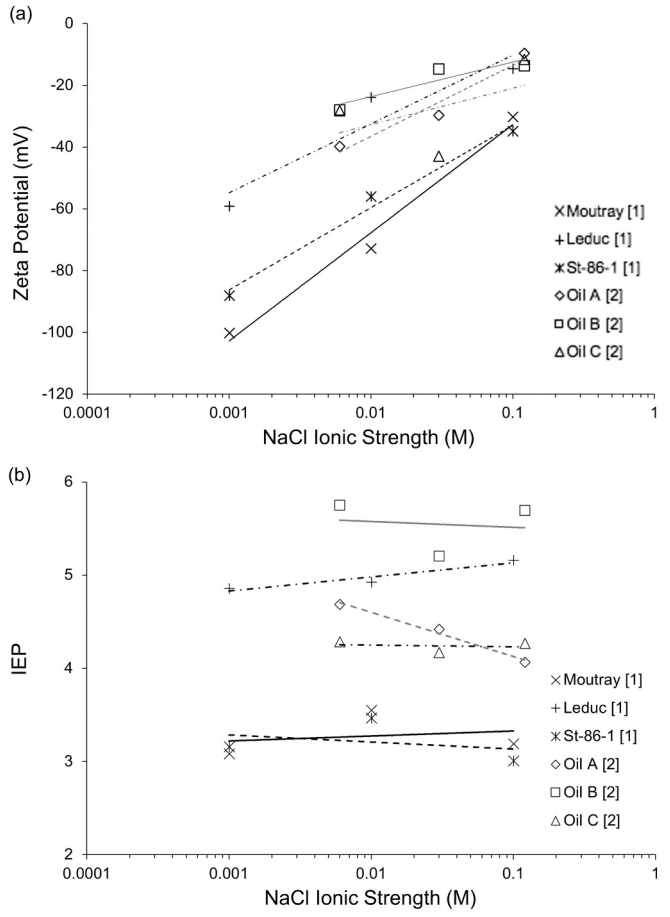

Fig. 6. Impact of ionic strength on measured zeta potential of crude oil emulsions in NaCl electrolyte. (a) zeta potential as a function of NaCl ionic strength at pH 6. (b) IEP expressed as pH as a function of ionic strength for different oils in NaCl electrolytes. Data from [1] Buckley et al. [18] [2] Kolltveit [55]. Dashed lines denote linear fit to the data, chosen in the absence of a strong theoretical basis to support higher order regressions.

reported a correlation between the change in zeta potential and wettability alteration in a different high salinity reservoir brine (FMB, Table 2). Of the eight crude oils tested in these studies, four yielded an increasingly negative zeta potential after wettability alteration to become more oil-wet, consistent with a negative zeta potential on the crude oil surface (Fig. 10; see [23]). Three crude oils yielded an increasingly positive zeta potential, consistent with a positive zeta potential on the crude oil surface. One crude oil yielded either a positive or negative change in zeta potential, depending on the host rock type. Collini et al. [24] interpreted these results to suggest that positive zeta potentials on crude oils in contact with natural brines are more common than previously thought based on the limited available data obtained using the EPM method (Fig. 7). However, the approach does not provide a direct measurement of the crude oil zeta potential and thus the magnitude of the zeta potential cannot be determined.

4.2. Direct measurements of zeta potential using the SPM

Here we test the hypothesis that oil-wet surfaces return the zeta potential of the wetting oil, rather than the underlying solid substrate ([23,24,49,50]; Fig. 1). We treat the mineral surfaces of natural sandstone substrates to render them strongly hydrophobic. These substrates are then coated with various crude oils and the zeta potential measured using the SPM and NaCl/$CaCl_2$ electrolytes up to 2 M ionic strength. The results are compared at lower ionic strength (10^{-3} and 0.02 M) against zeta potential measurements obtained using the EPM approach. We investigate the impact of varying pCa, because the impact of pH has been more extensively investigated and it is relatively straightforward to vary pH in EPM measurements (Fig. 2). In contrast, there are far fewer data available to characterise the impact of varying pCa, particularly at high Ca concentration and in high ionic strength electrolytes (Fig. 4). We focus here on exploring this parameter space.

4.2.1. Materials & methods

4.2.1.1. Substrate preparation. The porous media comprising the solid substrate were cylindrical cores of Fontainebleau sandstone (D = 3.7 cm; L = 7.6 cm; see Table 4), chosen primarily for its high quartz purity and chemical homogeneity (>99.9% SiO_2). Additionally, the permeability of the samples is high enough to allow for relatively rapid fluid saturation, whilst being low enough to generate a significant pressure drop during streaming potential measurements without having to apply high flowrates.

The Fontainebleau samples were cleaned with toluene and methanol using a Soxhlet apparatus and dried. The samples were then saturated with 5% di-methyl-di-chloridesilane in heptane (Silanization Solution-1, Sigma Aldrich) under a ca. 10^5 Pa vacuum pressure (negative pressure relative to atmospheric) for at least 24 h. Previous studies have used silanes to create strongly oil-wet natural sandstone samples [40]. The samples were then allowed to air dry at room temperature to remove excess solvent until a constant mass was obtained (typically after 24–48 h). Typical values of porosity and permeability after silanising were 6% and 185 mD (1.83×10^{-13} m^2) respectively (Table 4). The silanised samples were then saturated again under a ca. 10^5 Pa vacuum pressure with the crude oil of interest for at least 48 h.

The wettability of the silanised and oil-coated samples was characterised using the Amott water wetting index (Eq. (4.2)). Samples were submerged in a 10^{-3} M NaCl electrolyte for three weeks and the volume of electrolyte spontaneously imbibed (V_{WSI}) measured. In all cases, no electrolyte was imbibed, yielding an I_w value of zero, thus confirming the mineral surfaces of the silanised samples were strongly oil wet. Furthermore, droplets of water placed onto the outer surface of the silanised samples were not observed to spread, providing further indication of oil-wetting.

Following spontaneous imbibition, the silanised, oil-saturated samples were flooded with a 10^{-3} M NaCl electrolyte at a low rate (0.01 mL/min) for several days until no oil was observed in the effluent. High flowrate 'bumps' were then performed (up to 30 mL/min) to ensure all mobile oil was displaced. This process was repeated in the other direction of flow to ensure all mobile oil was flushed from the sample. Approximately 20% of the initial oil typically remained in the core and the sample permeability at the residual oil saturation was typically 50 mD (Table 4).

Fig. 11 shows a schematic of a pore/channel within a silanised and crude oil coated, Fontainebleau sandstone following our preparation method. Silanes react with the SiOH/SiO surface groups of the sandstone and the exposed methyl groups render the surface oil-wetting. When saturated with crude oil, the oil spreads over the silane surface and the residual oil that remains after displacement by the electrolyte exists as a thin wetting film (or order nanometers) on the flat portions of the mineral surfaces, and thicker layers (of order micrometers) in the corners of the pore-space. It is likely that some smaller pores remain entirely occupied by oil. During streaming potential measurements, the excess charge transported by the flowing electrolyte arises due to the electrical double layer at the crude oil interface (Fig. 1c).

4.2.1.2. Electrolyte ionic strength and composition. Electrolytes were prepared using deionised water and reagent grade salts (Sigma-Aldrich) to the desired ionic strength and composition. Electrolyte conductivity and pH were measured before and after experiments to ensure

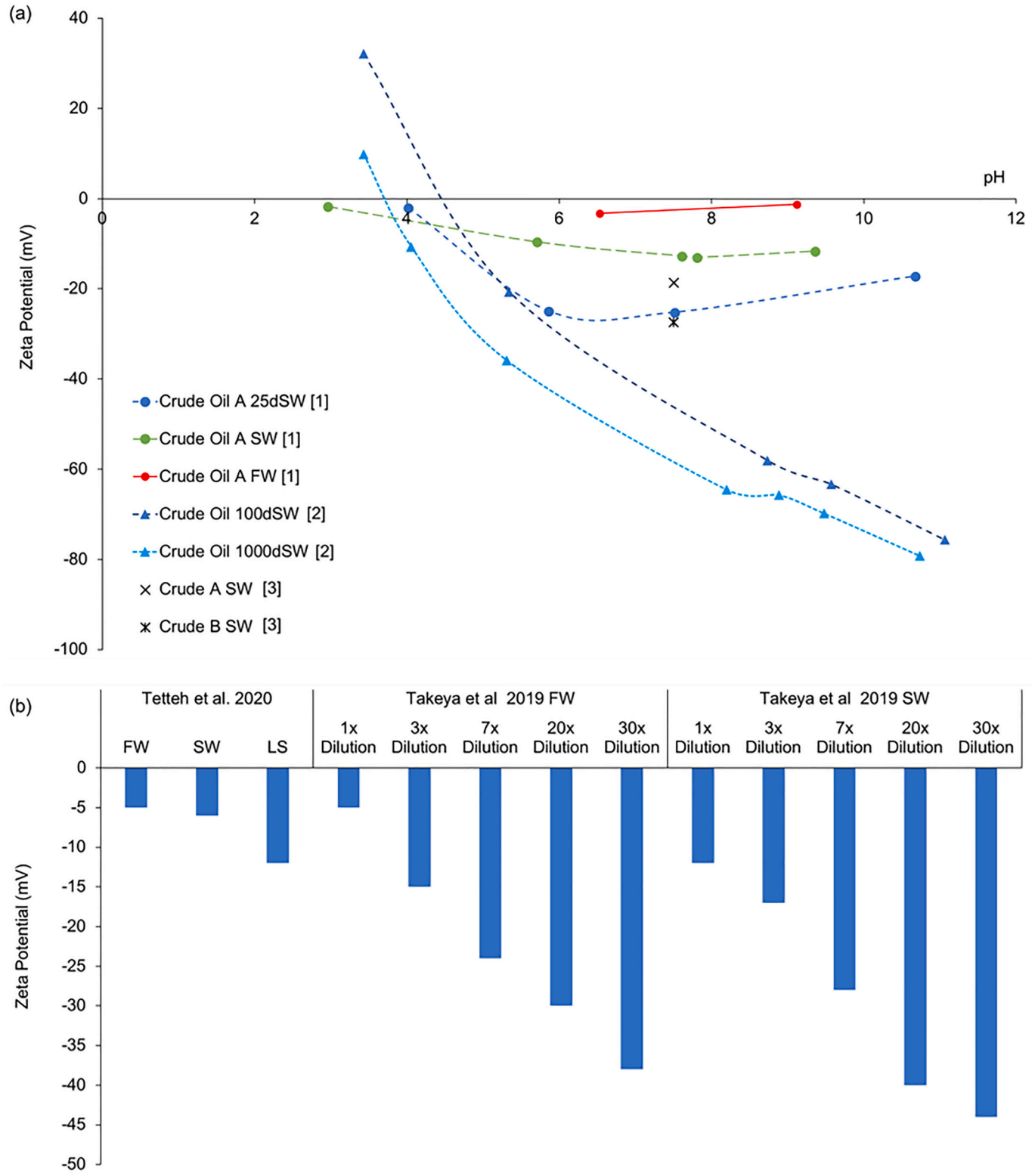

Fig. 7. Published zeta potential data measured on crude oil emulsions in complex electrolytes containing mixtures of ionic species representative of natural subsurface brines. Plot (a) shows data as a function of pH where this was reported by [1] Mahani et al. [64] [2] Alshakhs and Kovscek [5] [3] Mehraban et al. [67]. Plot (b) shows data where the pH was not reported from Tetteh et al. [87], Takeya et al. [85] and Takeya et al. [86].

consistency using a Metrohm 856 conductivity probe and a Mettler Toledo pH electrode respectively. No attempt was made to control pH but measured values remained within the range 5–6 across all experiments, irrespective of electrolyte composition and ionic strength, and the crude oil wetting the substrate. The zeta potential was measured using electrolytes containing NaCl and $CaCl_2$ salts of varying concentration, but ensuring the total ionic strength of each electrolyte was constant at a value of either 10^{-3} M; 0.02 M; 0.5 M or 2 M. The ionic strength was fixed for a given mixture of NaCl and $CaCl_2$ salts to ensure the contribution of ion interactions with the crude oil interface could be

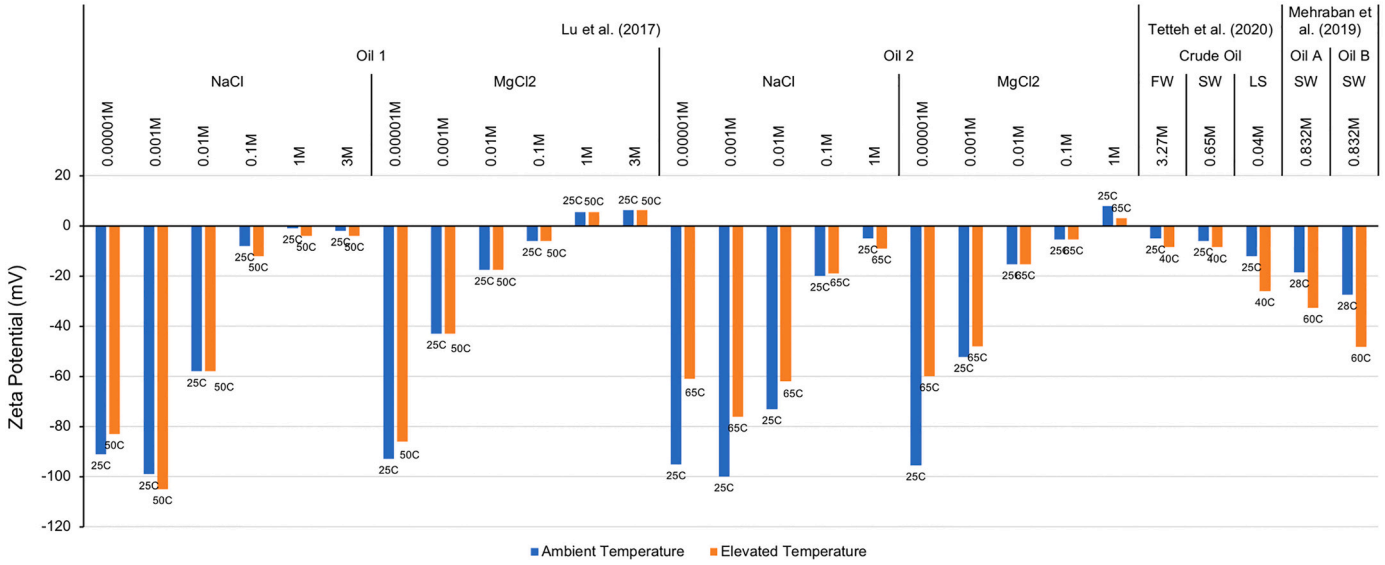

Fig. 8. Zeta potential data measured on crude oil emulsions in electrolytes at ambient laboratory (blue bars) and elevated (orange bars) temperature. Data labels report the measurement temperature. The relevant study, oil and electrolyte composition and ionic strength are listed. Electrolytes containing mixtures of ionic species that represent brines encountered in natural environments are shown as FW (formation water), SW (seawater), and LS (low salinity electrolyte) (see Table 2). Data from Tetteh et al. [87]; Mehraban et al. [67] and Lu et al. [62]. For a given value of ionic strength, the left hand column shows data at ambient temperature (blue in web version) and the right hand column shows data at elevated temperature (orange in web version).

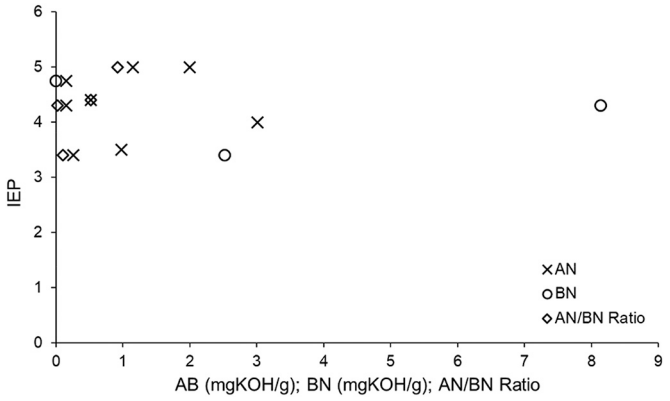

Fig. 9. Iso-electric point as a function of AN (crosses) BN (circles) and AN/BN Ratio (diamonds) for different crude oils. Data obtained from Buckley et al. [18]; Kolltveit [55]; Alshakhs and Kovscek [5] and Mahani et al. [63,64].

quantified, independent from the effect of varying total ionic strength. Streaming potential measurements for each sample and electrolyte ionic strength were performed initially with 10^{-3} M NaCl, and then with electrolytes with the same total ionic strength but increasing $CaCl_2$ concentration, in the order low to high total ionic strength. Completing the measurements in this sequence minimises the risk of Ca^{2+} adsorption during earlier experiments modifying the behaviour in later experiments.

4.2.1.3. Crude oil composition. Table 5 shows the properties of the five crude oils used in this study including the saturated aromatics, resins and asphaltenes (SARA) data.

4.2.1.4. SPM measurements. The SPM of Vinogradov et al. [89] was used to determine the zeta potential of the oil-wet samples; the apparatus and method have been used and reported in many previous studies (e.g. [3,4,24,50,89–91]) so are not described in detail here. An external pump was used to induce electrolyte flow through the sample and the pressure and voltage difference across the core were measured. The flow was allowed to stabilise before the pressure and voltage differences were recorded; this was repeated for typically five to eight different flow rates per streaming potential measurement. The direction of electrolyte flow through the sample was reversed at each flow rate to confirm the pressure and voltage responses were symmetric with respect to flow direction, ensuring there were no electrode polarisation effects.

Plotting the values of stabilised voltage difference against the values of stabilised pressure difference for each flow rate allows determination of the streaming potential coupling coefficient (C), given by the gradient of a linear regression through the data. The zeta potential was calculated using Eq. (2.3). Errors in the interpreted zeta potential were determined following the approach of Jackson and Vinogradov [50] and were typically of order ±1 mV. Following each streaming potential measurement, samples were re-saturated with the next electrolyte of interest by flooding the sample for at least 250 mL (>10 pore volumes) in both directions. Effluent pH and conductivity were measured to ensure consistency with the inlet values and varied by <5% for each experiment.

4.2.1.5. EPM measurements. Zeta potential measurements were also obtained using the EPM implemented in a Zetasizer NanoZS (Malvern Analytical) to compare against the SPM data. The same oils and electrolytes were used but only for total electrolyte ionic strength of 10^{-3} and 0.02 M for which it was possible to maintain a stable dispersion and obtain repeatable data. The zeta potential was measured using 15 runs per measurement and three measurements per sample. For each oil/electrolyte combination, two vials containing 20 mL of electrolyte and 4 droplets (ca. 0.1–0.2 mL) of crude oil were prepared. These were emulsified using a Turraxx Ultra stirrer at 10,000 rpm for 30 s. The emulsions were then left to settle for a few minutes before a 1 mL sample was drawn and inserted into the Zetasizer. Two samples from each vial were measured yielding a total of four samples and twelve zeta potential measurements per oil/electrolyte combination. The zeta potential reported is the average of these measurements ± two standard errors. Consistent with previous studies, the zeta potential was determined using Eq. (2.1).

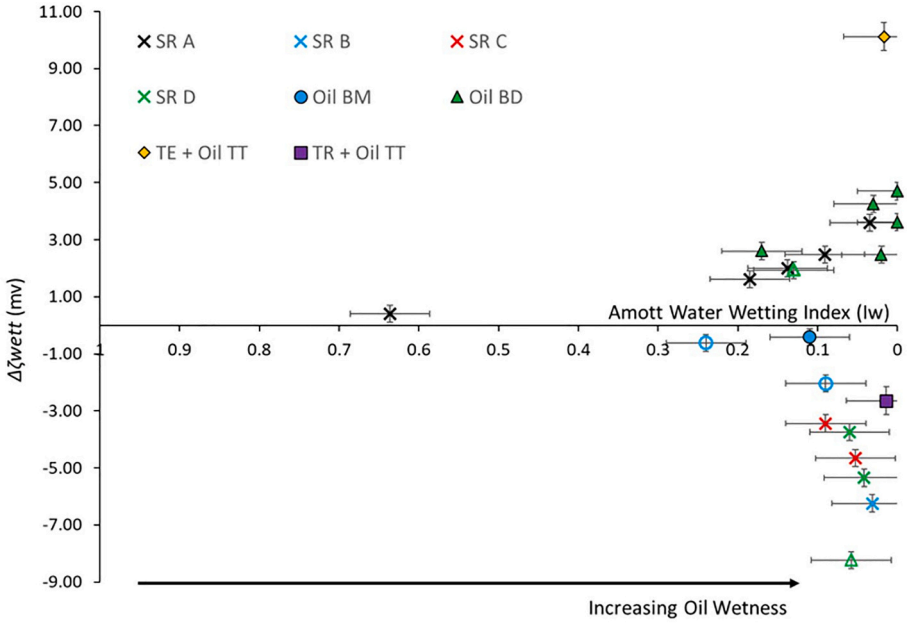

Fig. 10. Change in the zeta potential of brine-saturated carbonate rock samples after wettability alteration with crude oil ($\Delta wett$), plotted against the Amott water wetting index. Data from Collini et al. [24]. Different symbols represent the different crude oils. Filled symbols represent zeta potential measurements performed at ambient laboratory temperature (25 °C); empty symbols represent zeta potential measurements performed at elevated temperatures between 70 °C and 80 °C. Data showing positive values of $\Delta\zeta_{wett}$ were interpreted to reflect a positive zeta potential at the oil-brine interface whilst data showing negative values of $\Delta\zeta_{wett}$ were interpreted to reflect a negative zeta potential at the oil-brine interface.

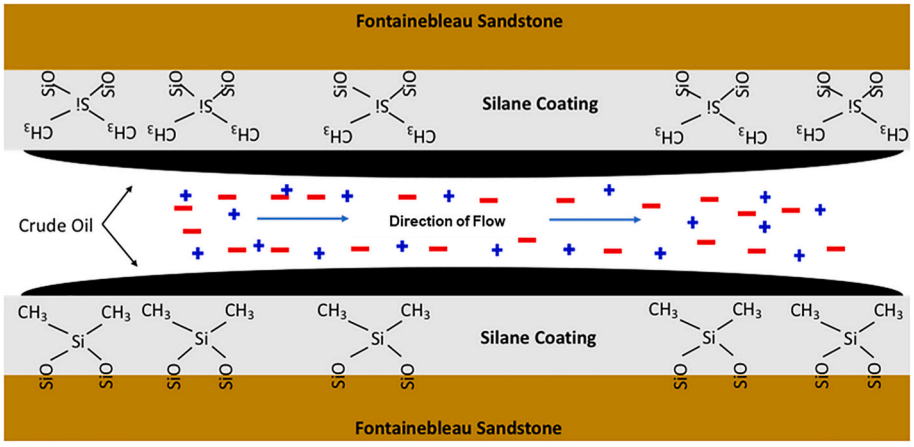

Fig. 11. Schematic of a pore within a crude oil coated, silanised, Fontainebleau sandstone sample. The excess charge transported by the electrolyte flow originates from the crude oil interface due to the strongly oil-wetting nature of the neutral substrate.

4.2.2. Results

4.2.2.1. SPM measurements. Fig. 12 reports zeta potential as a function of the percentage contribution of Ca^{2+} to the total ionic strength. The zeta potential becomes smaller in magnitude with increasing total ionic strength and increasingly positive with increasing Ca^{2+} concentration. However, the magnitude of the zeta potential varies between the different crude oils tested. The zeta potential ranges between ca. -50 mV (Oils BP/BM) and ca. -90 mV (Oil BD) in pure 10^{-3} M NaCl electrolyte (datapoints on the left-hand side of each plot), and between ca. -40 mV (Oil TT) and ca. -60 mV (Oil BM) in pure 10^{-3} M $CaCl_2$ electrolyte (datapoints on the right-hand side of each plot). The magnitudes of these zeta potential measurements are comparable to those reported previously for crude oil emulsions in similar electrolytes (Fig. 4). A full comparison between the zeta potential measurements in Fig. 12 and those previously published is presented later.

At high (2 M) ionic strength, which has not been tested previously, the measured zeta potentials are less negative and smaller in magnitude, ranging between ca. -20 mV (oil BM) and ca. -10 mV (oil TT) in pure NaCl electrolyte, and ca. -1 mV and ca. +0.6 mV (oil TT) in pure $CaCl_2$ electrolyte. The zeta potential measurements were negative in all but this latter case; the concentration corresponds to a pCa of 0.17, similar to the concentration at which positive zeta potential measurements have been observed previously (Fig. 4). We are confident in the polarity of this measurement because the gradient of the linear regression between stabilised values of ΔV and ΔP (Eq. (2.2)) shows a clear change from negative to positive.

The zeta potential results reported in Fig. 12 are shown in Fig. 13 plotted as a function of pCa. For all samples, and for each value of total electrolyte ionic strength, there is a clear linear relationship between zeta potential and pCa as observed previously (Fig. 4). The gradient of the linear trend decreases with increasing total ionic strength, confirming that the sensitivity of the zeta potential to Ca^{2+} decreases with increasing ionic strength. Note that the data shown here differ from most previous experimental measurements, because the total ionic strength remains constant for each suite of measurements (denoted by different symbols), rather than increasing with decreasing pCa. Hence, we can directly observe for the first time the effect of varying pCa, independent of the effect of varying total ionic strength.

These data are collated into one plot for cross comparison between

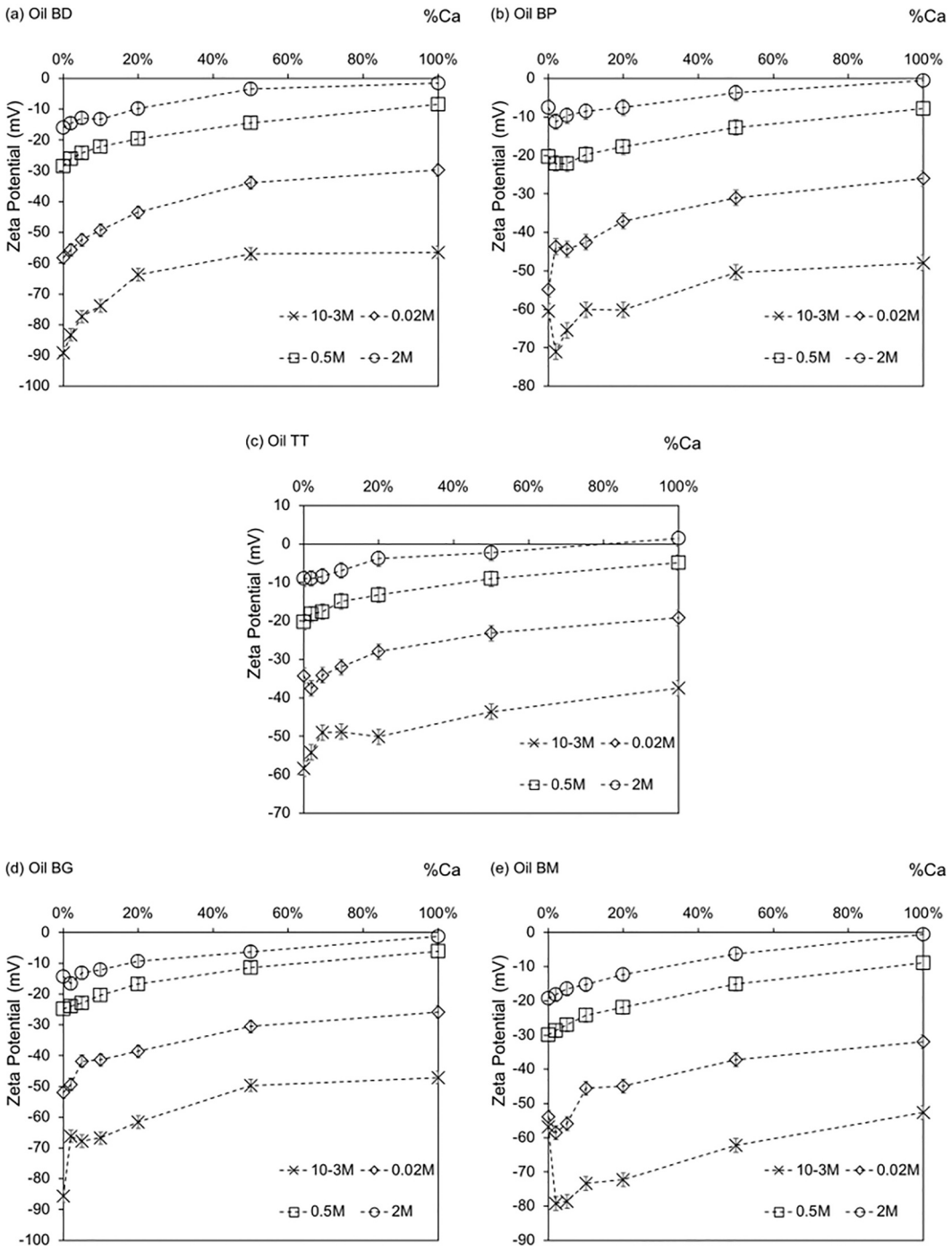

Fig. 12. Zeta potential as a function of Ca^{2+} percentage at constant ionic strength. Panels show different crude oils and the datasets on each panel correspond to different values of total ionic strength. Zeta potential determined using the SPM. Experimental errors are shown and are similar to the symbol size.

the different crude oils tested in Fig. 14. Linear trendlines are fitted to all the data for a given crude oil regardless of total electrolyte ionic strength. The variation in the trendlines between the different crude oils demonstrates their different zeta potential behaviour. Consistent with previous published data (Fig. 4), a linear relationship between the zeta potential and pCa is indicative of Nernstein behaviour and we can determine the Stern layer capacitance using Eq. (3.1), noting that the validity of the GCS model at high ionic strength has been questioned and it may not apply to the data obtained at 2 M ionic strength (e.g. [31]). However, a linear regression including only the data obtained at lower ionic strength also provides a good match to the high ionic strength data. Values of the Stern layer capacitance obtained from the regressions are reported in Table 3.

The Stern layer capacitance determined for these crude oils ranges from 1.54 F•m^{-2} for Oil TT to 3.97 F•m^{-2} for Oil BD. These values are similar to those obtained from previous measurements of zeta potential as a function of pCa, which range from 0.72 F•m^{-2} to 5.63 F•m^{-2} (Table 3). For comparison, Takeya et al. [85] used a value of 2.25 F•m^{-2} for the Stern layer capacitance in their model of the crude oil surface, which is close to the average value found here. The difference in the Stern layer capacitance for different crude oils suggests different surface properties and interaction with Ca^{2+}.

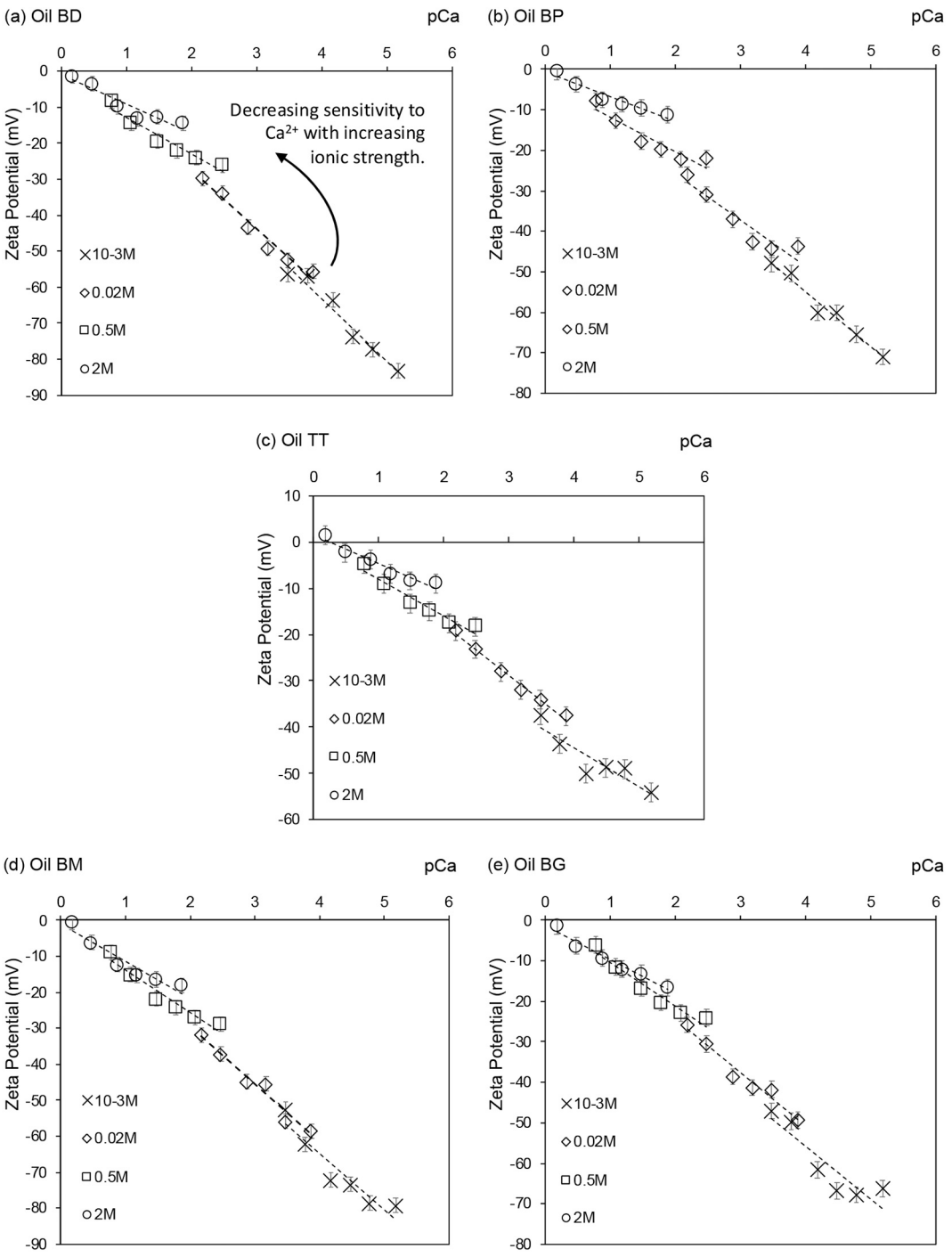

Fig. 13. Zeta potential measurements reported in Fig. 12 plotted as a function of pCa. Panels show different crude oils; the datasets on each panel correspond to different values of total ionic strength. Dashed lines denote linear fit to the data for the different values of electrolyte ionic strength.

4.2.2.2. Comparison of SPM and EPM measurements. Fig. 15 shows examples of the zeta potential distributions reported from the Zetasizer measurements. The software has a built-in test for normality that determines whether the data for a given distribution is 'good' or 'poor'. Fig. 15(a) and (b) show examples of 'good' distributions obtained on emulsions of Oil TT. A mean of -31 mV and a standard deviation of approximately 7.5 mV was obtained over the 15 sub-runs. These examples are typical of the better Zetasizer measurements obtained here and represent the lower end of the range of observed standard deviation. Oil TT typically produced the most stable emulsions and the most repeatable zeta potential data.

Conversely, Fig. 15(c) and (d) show examples of 'poor' zeta potential distributions. The data shown in (c) for an emulsion of Oil BG is highly scattered and shows a wide range of zeta potential, captured by the large standard deviation of 155 mV. Furthermore, the mean of this measurement (−27 mV) differs significantly from the mode (95 mV). Similarly, the data shown in Fig. 15(d) for an emulsion of Oil BP has a large standard deviation (70 mV). Considering the mean values alone, these measurements would appear reasonable by comparison with previous data (Fig. 4). However, it is clear from the distributions that the data here are poor quality. Finally, Fig. 15(e) and (f) show examples of measurements where the underlying distribution was deemed 'good' but

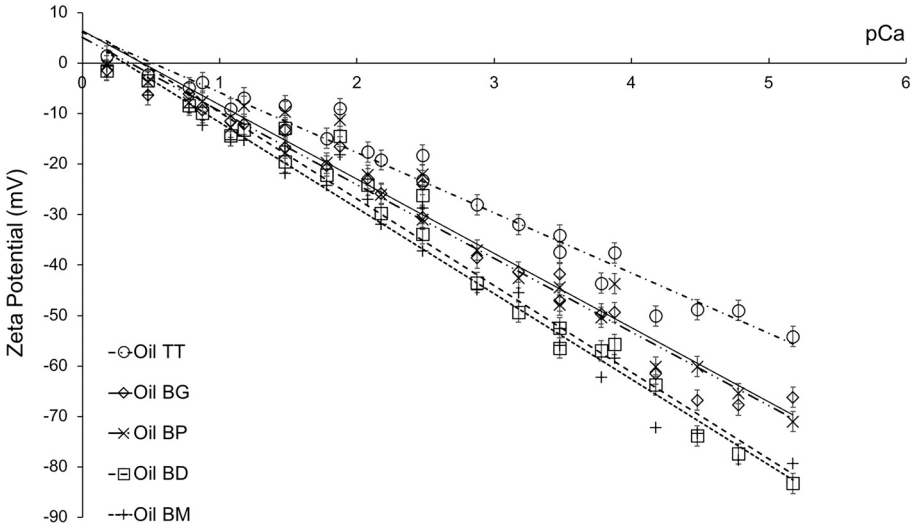

Fig. 14. Zeta potential measurements as a function of pCa for all crude oils tested here. Dashed lines denote best fit linear regression to all data for a given crude oil, irrespective of total electrolyte ionic strength. Data extracted from Fig. 12.

there is an unacceptably broad range of values. Fig. 15(e) shows data from an emulsion of Oil BM and has a mean of −25 mV and a standard deviation of 15 mV, whilst Fig. 15(f) shows data from an emulsion with Oil BP with a mean of −57 mV and a standard deviation of 21 mV.

Results such as these were common in the experiments conducted here. However, considering only the 'summary results' of mean zeta potential, conductivity, and electrophoretic mobility provided by the software, it would not necessarily be clear that such a poor or broad underlying distribution was present. Fig. 15(c)-(f) highlight the challenges in measuring the zeta potential of emulsions of crude oil in aqueous electrolytes (see also [55]).

It has been reported that the volume of oil dispersed in the electrolyte, along with the droplet size, can significantly affect the interpreted value of the zeta potential, with increasing oil fraction and/or droplet size yielding a larger magnitude zeta potential [58,59,72]. The three more viscous oils (BP, BG and BM) tested here produced noticeably less stable emulsions than Oil TT. The broader distributions observed for these three oils may have been due to broader and more variable droplet size distributions within and between different measurements. Emulsions of Oil BD exhibited behaviour somewhere between Oil TT and Oils BP, BG and BM.

Zetasizer measurements on a given sample were generally consistent. However, different samples from the same emulsion could yield significantly different results, even if the underlying distribution was 'good'. Many previous studies have reported only the range in zeta potential measurements from a single sample [59,68,85,86]. In some studies, there is no discussion of repeat measurements. Conducting experiments in this way may underestimate the error in the zeta potential. Moreover, if the underlying distribution was not considered when analysing data, poor distributions such as those shown in Fig. 15c and d may have been reported as good results. The only study that discusses the reported distribution of measured zeta potential on crude oil is that of Kolltveit [55], who noted many of the same challenges discussed here.

It should be noted that streaming potential measurements do not yield insight into the microscale zeta potential distribution [23]. The measurements reported here correspond to a complex average of the zeta potential at individual interfaces within the porous medium. The SPM data are therefore compared to the mean zeta potential values interpreted from the EPM measurements. Fig. 16 compares these data for Oil TT which, as discussed above, was the only crude oil for which the Zetasizer produced good data.

A good match between the data obtained using the two experimental methods is observed, with the EPM data aligning well with the linear trendline fitted to the SPM data (Fig. 16). The consistency between the different measurement techniques provides confidence that the oil-coated silane substrates used in the SPM measurements return the zeta potential of the oil-electrolyte interface.

4.2.2.3. Relationship between zeta potential and crude oil properties. The new data reported here determine the zeta potential and associated properties for five crude oils that have not been investigated previously, using a consistent experimental method and conditions, allowing direct comparison and revealing a range of crude-oil dependent behaviour. In light of this, we test for any correlations between crude oil composition and zeta potential. Fig. 17 plots the zeta potential data obtained with pure NaCl and $CaCl_2$ electrolytes as a function of the crude oil AN, BN and AN/BN ratio. A weak correlation is apparent between zeta potential and AN for both electrolytes, with zeta potential becoming more positive with increasing AN. There is no similar trend for BN, so the trend of zeta potential with AN/BN ratio follows the AN trend. The apparent sensitivity to AN is higher for the NaCl electrolyte than the $CaCl_2$ electrolyte.

We also test for relationships between oil properties and the linear Nernstein relationship between zeta potential and pCa observed in Fig. 14, plotting the gradient of the trendlines shown in Fig. 14 against the oil AN, BN and AN/BN ratio. The intercept of the trendlines with the x-axis in Fig. 14 is also plotted; the intercept correlates to IEP expressed as pCa. There is again an apparent correlation between the gradient, and the IEP, with AN (Fig. 18a): the gradient and IEP both increase with increasing AN. The correlation with BN is again less clear, with a weak trend for decreasing IEP with increasing BN and no apparent correlation with gradient (Fig. 18b). The trend with AN/BN ratio largely follows the AN trend but is dominated by the large AN/BN ratio for oil TT (Fig. 18b).

5. Discussion

5.1. Development of surface charge on crude oil in aqueous solution

5.1.1. Adsorption of hydroxyl ion

The development of surface charge on non-polar fluids in aqueous solution has been widely interpreted to arise in response to the strong affinity of the hydroxyl ion for interfaces between water and hydrophobes [10,11,25,26,35,36,41,65,66,76,82]. Gray-Weale and Beattie [41] suggested that hydroxide ions are unusual because they reduce the relative permittivity of an electrolyte solution more than other monovalent, monatomic ions, suppressing the dipole-moment fluctuations of nearby water molecules which leads to a force acting on the hydroxide

Table 3
Gradient of the linear regression between zeta potential and pH or pPDI fitted to measured data close to the IEP, and the Stern layer capacitance calculated from the gradient using the simple Gouy-Chapman-Grahame model (Eq. (3.1)), for various crude and non-polar oils and aqueous electrolytes reported in the literature and for the new data reported here.

Oil [source reference]	Ionic strength (M)	pH	PDI	Gradient (mV/decade)	Stern layer capacitance (F/m^2)
Impact of pH in NaCl electrolyte (Figs. 2, 3):					
Moutray [Buckley et al. [18]]	0.1			−10.5	0.16
Moutray [Buckley et al. [18]]	0.01			−24.5	0.17
Moutray [Buckley et al. [18]]	0.001			−37.3	0.13
Leduc [Buckley et al. [18]]	0.1			−12.7	0.21
Leduc [Buckley et al. [18]]	0.01			−24.6	0.17
Leduc [Buckley et al. [18]]	0.001			−38.6	0.14
C9-C16 Alkanes [Stachurski and Michalek [82]]	0.001			−19.0	0.04
Impact of pCa and pMg (Figs. 4, 14):					
Moutray [Chow et al. [21]]		10	Ca	−23.3	4.51
Moutray [Chow et al. [21]]		4	Ca	−6.37	0.72
Crude Oil [Takeya et al. [85]]		8	Ca	−22.8	5.63
Crude Oil [Takeya et al. [85]]		10	Ca	−18.5	4.11
Crude Oil [Takeya et al. [85]]		8	Mg	−8.88	0.92
Oil A [Takeya et al. [86]]		8	Ca	−22.6	5.00
Oil B [Takeya et al. [86]]		8	Ca	−24.5	5.52
Oil C [Takeya et al. [86]]		8	Ca	−25.9	5.91
Oil D [Takeya et al. [86]]		8	Ca	−25.8	5.88
Oil A [Takeya et al. [86]]		8	Mg	−24.5	5.52
Oil B [Takeya et al. [86]]		8	Mg	−25.0	5.66
Oil C [Takeya et al. [86]]		8	Mg	−24.0	5.38
Oil D [Takeya et al. [86]]		8	Mg	−23.5	5.25
Docosane [Dunstan & Saville [32]]		N/A	Ca	−9.30	0.78
BD [This Study]		5.5	Ca	−17.0	3.97
BM [This Study]		5.5	Ca	−17.2	3.54
BG [This Study]		5.5	Ca	−14.7	2.50
TT [This Study]		5.5	Ca	−11.9	1.54
BP [This Study]		5.5	Ca	−14.6	2.73

Table 4
Petrophysical properties of the substrates used in the SPM measurements.

	Fontainebleau (FB)	Silane coated FB	Oil and silane coated FB
Length (cm)	7.6	7.6	7.6
Diameter (cm)	3.7	3.7	3.7
Porosity (%)	10	8	8
Water Permeability (mD)/(m^2)	$200/1.97 \times 10^{-13}$	$185/1.83 \times 10^{-13}$	$50/4.93 \times 10^{-14}$
Oil Saturation (%)	N/A	N/A	20

ion that attracts it to regions of low permittivity. They used this model to reproduce the pH dependence of zeta potential (e.g. Fig. 3). Roger and Cabane [76] suggested that hydroxide adsorption at hydrophobic interfaces was energetically unfavourable and suggested instead that hydroxide ions react with trace amounts of fatty acids. They used this model to explain the dependence of zeta potential and emulsion interfacial area on subtle changes in oil purity. Creux et al. [25] suggested that hydroxide adsorption dominates until very low pH (2–3 in their experiments), at which point proton adsorption becomes sufficiently significant to yield positively charged hydrophobic interfaces. Uematsu et al. [88] show that interfacial adsorption of small inorganic ions such as the hydroxyl ion cannot account for the experimentally measured zeta potential of hydrophobic surfaces and suggest instead the presence of very small concentrations of interfacially active impurities (weak acids and basis) in the water.

Whatever the underlying cause, the consistent behaviour observed for non-polar oils and other hydrophobes suggests the magnitude and polarity of the surface charge is controlled only by the electrolyte properties ([66]; Fig. 3) and the available data suggest that the concentration of the hydroxide ion plays a key role [41,76]. However, adsorption of hydroxide ions alone cannot explain the dependence of the zeta potential on multivalent ion concentration (Fig. 5), which Dunstan and Saville [32] suggested to be caused by preferential solubility of ions in the interfacial region. Moreover, our collated data show that crude oils display far more variable zeta potential behaviour for given electrolyte pH, composition and ionic strength than non-polar oils. This variability suggests that properties of the crude oil also play a role in controlling the development of surface charge.

5.1.2. *Interfacially-active polar organic molecules*

Crude oils contain a broad range of non-polar, polarizable and polar organic species, including hydrocarbons, asphaltenes, resins, paraffins, sulfuric species and ash/residue [81]. The types and quantities of these species are highly variable across different crude oils. Fluid-fluid interfaces are dynamic in the sense that species can migrate from the bulk fluid to the interface and vice-versa [1,81]. Organic molecules may also partition into the aqueous phase and vice-versa. The interfacial region may therefore be highly complex and dynamic, and contain acid and base impurities derived from the crude oil itself that are interfacially-active [12,43,47].

Experimental data suggest asphaltenes and resins play an important role in stabilising aqueous emulsions of crude oil, and the wetting of solid surfaces by crude oil in aqueous solution, which suggests that these molecules are interfacially-active and contribute to the development of surface charge [1,16,17,33,54,83]. It has been suggested that asphaltenes become electrically charged due to the dissociation of carboxylic acid groups and/or the protonation of hydroxyl and basic amine groups [1,16,18,30,54,83].

Asphaltenes are typically defined and measured as the proportion of crude oil components that are soluble in aromatic solvents but precipitate in alkane solvents [1]. Atomic force microscopy (AFM) data have been interpreted to suggest that asphaltenes in crude oil are adsorbed at the interface with an aqueous electrolyte, yielding more negative surface electrical charge as compared to asphaltene-free oil [79,80]. Solid asphaltenes, precipitated from crude oils, have been shown to develop surface charge in aqueous solution; the corresponding zeta potential is pH dependent and displays similar behaviour to that of crude oils: at low pH the zeta potential is positive and becomes increasingly negative with increasing pH [73,83]. However, bulk measurements of asphaltene content in crude oil yield little insight into interfacial properties; indeed, several studies have found that bulk asphaltene content is a poor indicator of emulsion stability and wetting behaviour [16,27,95]. The proportion of asphaltenes that are interfacially-active is unclear and may be highly dynamic: Chaverot et al. [19] estimate 0.015% of the bulk, whilst Yang et al. [95] suggest a much higher figure of 2%. Yang et al. [94] showed that interfacially-active asphaltenes have a higher molecular

Table 5
Bulk fluid properties for the crude oils used in this study.

Oil	Acid number (mgKOH/g)	Base number (mgKOH/g)	Saturates (%)	Aromatics (%)	Resins (%)	Asphaltenes (%)	Total resins + asphaltenes (%)
BM	0.01	2.00	16.8	50.0	23.2	7.10	30.2
BG	0.05	0.60	22.0	41.0	20.0	17.0	37.0
BP	0.19	2.60	30.0	34.0	25.0	11.0	36.0
BD	0.20	1.80	43.5	46.0	10.1	0.40	10.5
TT	0.34	0.41	48.4	48.1	2.80	0.70	3.50

Table 6
Surface complexation reactions (SCM) and associated equilibrium constants used by Bonto et al. [13] to model experimental zeta potential data for crude oils in aqueous electrolytes.

Reaction number	Surface site	Reaction	Log (k)
1	>NH (Amine Base)	$>NH + H^+ \rightarrow > NH_2^+$	7.27
2	>COOH (Carboxylic Acid)	$>COOH \rightarrow > COO^- + H^+$	−4.62
3		$>COOH + Ca^{2+} \rightarrow > COO\text{-}Ca^+ + H^+$	−3.30
4		$>COOH + Mg^{2+} \rightarrow > COO\text{-}Mg^+ + H^+$	−3.30
5		$>COOH + Na^+ \rightarrow > COO\text{-}Na + H^+$	−3.40
6	>wOH (Weak Non-Polar)	$>wOH \rightarrow > wO^- + H^+$	−6.23
7		$>wOH + Na^+ \rightarrow > wO\text{-}Na + H^+$	−5.70
8		$>wOH + Ca^{2+} \rightarrow > wO\text{-}Ca^+ + H^+$	−4.60
9		$>wOH + Mg^{2+} \rightarrow > wO\text{-}Mg^+ + H^+$	−4.60

weight and oxygen content than those in the bulk, suggesting the structure of the asphaltene may also be important in controlling interfacial properties.

It has also been suggested that acid and base hydrocarbon molecules (those with carboxylic acid or amine functional groups) are interfacially-active (e.g. [78]) and that these molecules can develop an electrical charge through dissociation and protonation of the acid and base groups respectively [18,30,33]. The interfacial behaviour of acidic hydrocarbon compounds has received comparatively more attention. The concentration of acids at the interface of crude oil in aqueous electrolytes has been shown to be higher than in the bulk [7,42]. Evidence of increased emulsion stability [43,77] and reduced oil-water interfacial tension (IFT; [47]) with increased bulk acid concentration further suggest acids are interfacially-active. Measured changes in oil-water IFT have also been interpreted to suggest that base hydrocarbon compounds are less interfacially-active than acids [12,48,69]. As with asphaltenes, it is unclear what proportion of bulk acids or bases will be interfacially-active for a given crude oil composition.

5.1.3. Surface complexation models for the crude-oil surface in aqueous solution

Motivated by these observations, several studies have developed surface complexation models (SCM) for crude-oil in aqueous solution, in which it is assumed that dissociation of acid groups and protonation of base groups present at the interface leads to the development of surface charge ([13,14,20,21,28,85]; reactions 1 and 2 in Table 6). These models further assume that acid sites can react with divalent cations ([13,14,85]; reactions 3 and 4 in Table 6). Bonto et al. [13] noted the role of the hydroxyl ion in developing surface charge on non-polar oils and added a further reaction with so-called 'weak sites' that attempted to account for this (reaction 6 in Table 6). Despite this additional reaction, the fit to measured data was poor and additional reactions were added between acid sites and Na^+ (reaction 5 in Table 6) and between the 'weak' sites and Na^+, Ca^{2+} and Mg^{2+} (reactions 7–9 in Table 6). Bonto et al. [13] pointed out that these additional reactions need to be tested in experiments, but their inclusion improved the model fit to the experimental data of Buckley et al. [18] and Kolltveit [55] shown in Fig. 2.

SCMs based on the reactions shown in Table 6 predict that surface acid sites and divalent cations are pH dependent, consistent with measured zeta potential data (Fig. 4). Fig. 19a and b show the predicted proportion of negatively-charged, neutral and positively-charged surface acid sites as a function of pPDI and pH. Plot (b) shows the impact of varying pCa whilst plot (c) shows the impact of pMg for two different values of pH. The curves are similar for both cations due to the similarity of the equilibrium constants (Table 6). At pH 4, only a small fraction of the surface sites are negatively charged across the range of pCa or pMg (pPDI). Almost all sites are neutrally charged at high pPDI and a fraction of these become positively charged as pPDI decreases. Conversely, at pH 7, most of the sites are negatively charged at high pPDI whilst some are neutrally charged. This is consistent with the more negative zeta potential data at pH 7 compared to pH 4 observed in the low pPDI range (Fig. 4). Decreasing pPDI results in an increasing proportion of the surface sites becoming positively charged, consistent with increasingly positive zeta potential (Fig. 4). The proportion of sites that are positively charged changes over a much broader pPDI range at pH 7 than pH 4, indicating increased sensitivity of the surface charge to divalent cations at higher pH.

A key problem with such SCMs for crude-oil in aqueous solution is determination of the surface site density. Adsorption of hydroxyl ions has been interpreted to yield a surface site density of ca. 3/nm^2 irrespective of the oil (e.g. [26]) and this value was used for the 'weak' sites in the SCM of Bonto et al. [13]. However, the density of acid and base sites is poorly constrained. Some approaches have adjusted the acid and base site density as part of the match to experimental data (e.g. [18,21]); others have attempted to predict the surface site density using bulk oil properties such as AN and BN (e.g. [13]). The presence of acid and base sites at the interface is plausible, given the evidence that these species are interfacially-active. However, the site density is unlikely to be constant at dynamic fluid-fluid interfaces even for a given crude oil; moreover, the distribution of acid and base species may be affected by the development of an EDL on the crude-oil side of the interface, in which case the surface site density may depend on the electrolyte properties in addition to the oil properties.

The zeta potential data collated here highlight some key features that models for the development of surface charge on crude oil must capture. First, different crude oils return different values of zeta potential for given values of pH, divalent ion concentration and total electrolyte ionic strength; they also show different sensitivity to variations in pH and ion concentration. Furthermore, crude oil zeta potentials and their sensitivity to pH and electrolyte composition are different to those observed using non-polar oils and other hydrophobes. The variability across different crude oils is in marked contrast to the consistent behaviour observed for non-polar oils; taken together, the evidence suggests that controls on the development of charge on the crude oil surface in aqueous solution are not restricted to the properties of the electrolyte, as has been suggested for non-polar oils, but also depend on properties of the crude oil [33,85,86].

Second, crude oils consistently show close-to-linear (Nernstian) variation in zeta potential with pH and pCa, close to the IEP. Non-polar oils also show close-to-linear behaviour; however, the Stern layer capacitance, interpreted using the simple GCS model, is consistently

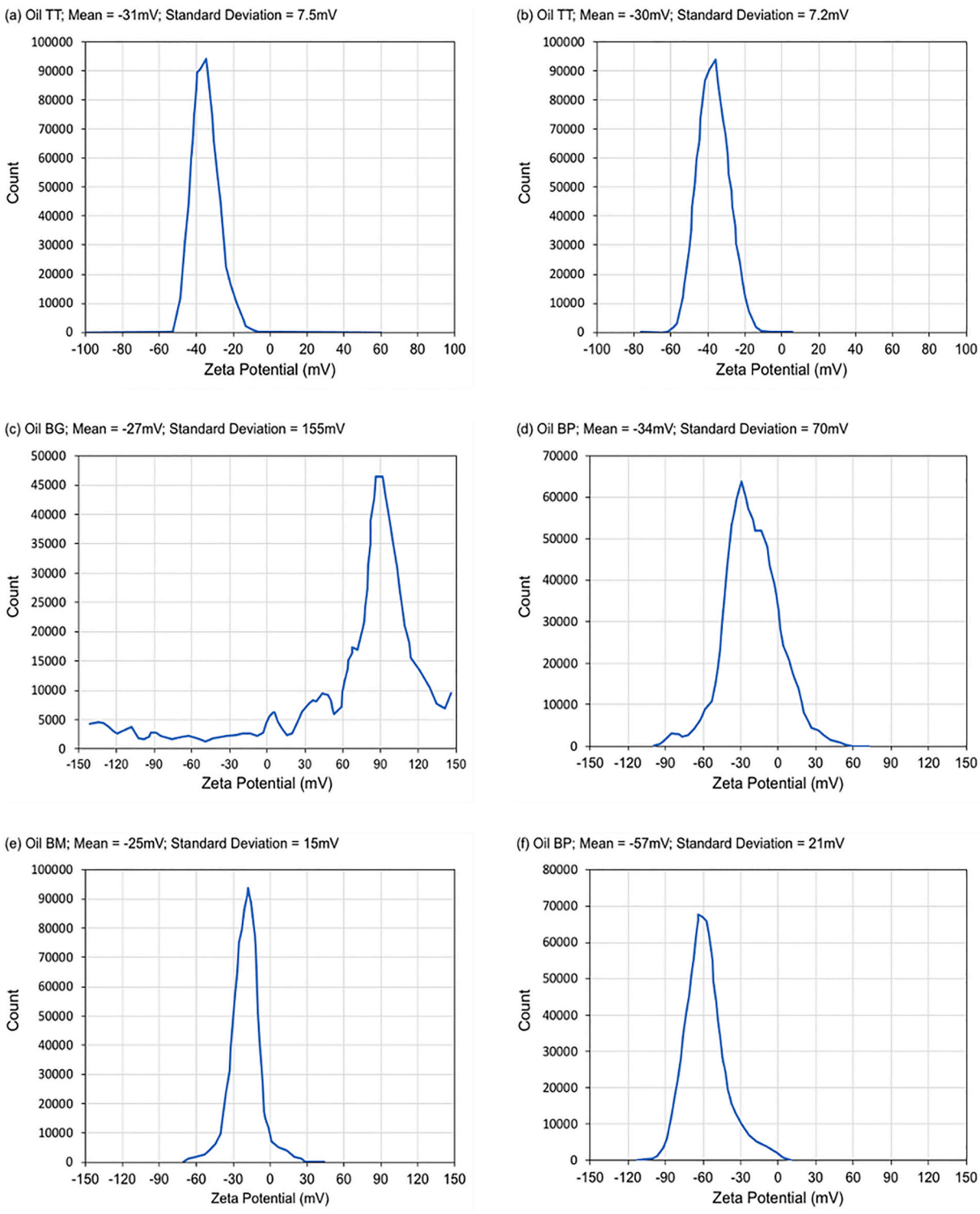

Fig. 15. Examples of the zeta potential distributions obtained from Zetasizer measurements on oil-electrolyte emulsions. (a) Oil TT; Mean = −31 mV; Std. dev. = 7.5 mV (b) Oil TT; Mean = −30 mV; Std. dev. = 7.2 mV (c) Oil BG; Mean = −27 mV; Std. dev. = 155 mV (d) Oil BP; Mean = −34 mV; Std. dev. = 70 mV (e) Oil BM; Mean = −25 mV; Std. dev. = 15 mV (f) Oil BP; Mean = −57 mV; Std. dev. = 21 mV.

larger for crude oils as compared to non-polar oils and is also variable across different crude oils for similar electrolyte pH and/or divalent ion concentration. These data suggest that the density of immobile excess charge at the crude oil interface is higher than for non-polar oils; this excess charge may be adsorbed on the crude oil surface (e.g. [14]) and/or be preferentially less soluble in the interfacial region (e.g. [32]) and/or reflect the presence of interfacially-active impurities in the water that could be derived from the oil (e.g. [88]).

Third, crude oils show charge inversion in NaCl electrolytes at low pH, and in $CaCl_2$ electrolytes at low pCa, switching from negative to positive values with decreasing pH and pCa. Charge inversion in these electrolytes has not been observed for non-polar hydrocarbons; Creux et al. [25] observed positive zeta potential for octane, decane and dodecane in aqueous solution, with the IEP in the range pH 2–3, but no

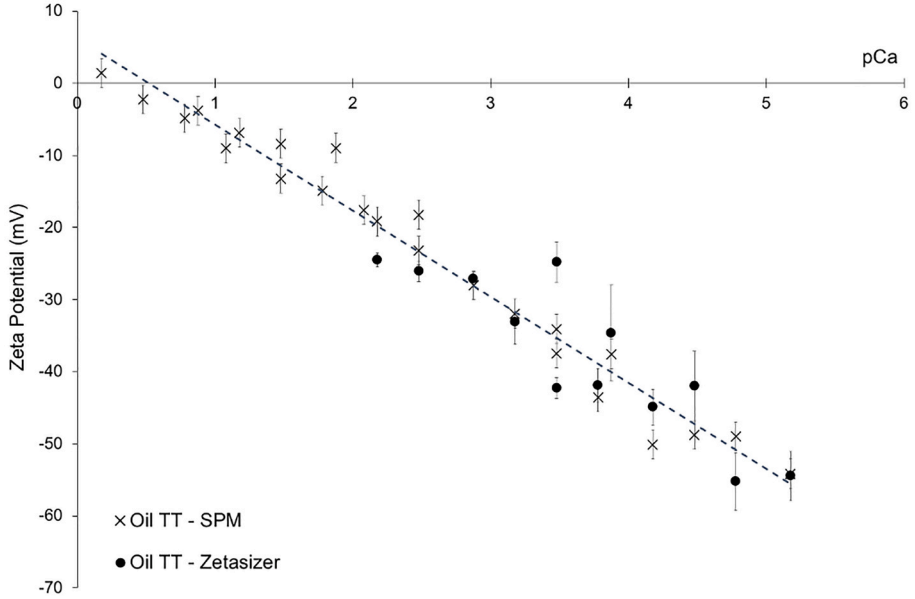

Fig. 16. Comparison of streaming potential measurements and Zetasizer measurements of the zeta potential of Oil TT as a function of pCa. SPM data extracted from Fig. 12. Dashed line denotes linear fit to all data.

NaCl was added to their pure water electrolyte, so their data cannot be directly compared to those shown in Fig. 3. Dunstan and Saville [32] observed positive zeta potential on docosane in $AlCl_3$ electrolyte, but there are no comparable data for crude oils.

Finally, the new measurements of zeta potential reported here suggest a weak correlation between zeta potential and the AN of the crude oil for both NaCl and $CaCl_2$ electrolytes (Fig. 18). The apparent sensitivity to AN is higher for the NaCl electrolyte than the $CaCl_2$ electrolyte; the IEP in $CaCl_2$ electrolytes (expressed as pCa) also correlates with AN, as does the gradient of the linear regression between zeta potential and pH (NaCl electrolytes) and pCa ($CaCl_2$ electrolytes). These findings are consistent with the evidence that crude oil properties also control the development of surface charge in aqueous solution, and that polar acid species in crude oil are interfacially-active [86]. However, AN and BN are bulk properties and may have a weak or variable relationship with interfacial properties and presence and type of surface sites [86].

5.2. Measurement of crude oil zeta potential on wetting layers using the SPM

The zeta potential data obtained here on wetting crude oil layers using the SPM are consistent with the three main trends observed in previously published data obtained using the EPM and crude-oil emulsions (i) the zeta potential of the crude oil-electrolyte interface is typically negative at pH > 5 (ii) the magnitude of the zeta potential decreases with increasing ionic strength, and (iii) addition of Ca^{2+} yields a more positive zeta potential, with a strong linear correlation observed between the zeta potential and pCa indicating Nernstian behaviour. Fig. 20 directly compares the new data with the published data shown in Fig. 4. The gray shaded region represents the new data bounded by the steepest trendline (Oil BM) and the shallowest trendline (Oil TT). The small black crosses represent the individual data points in Fig. 14.

The new data show similar behaviour to those obtained previously, although it should be noted again that the data reported here were obtained at several different values of constant ionic strength, fixed by adjusting the concentration of Na^+, whereas the ionic strength of the published data increases with decreasing pCa. The new data were also obtained at higher ionic strength (up to 2 M) than previous studies; moreover, at pH 5–6, the new data occupy a parameter space that has been little explored previously, between low pH (pH 4) and high pH (pH > 7), that is relevant to many natural subsurface environments.

The data show that the sensitivity of the crude oil surface to Ca^{2+} is more significantly impacted by pH than the concentration of Na^+, with the sensitivity of the crude oil surface to Ca^{2+} increasing with increasing pH, consistent with the predictions of the few SCMs for crude oil as discussed in the previous section (Fig. 19). The data also show significant variability across different crude oils, with weak correlations between zeta potential and AN, and between IEP and AN as discussed in the previous section (Figs. 17, 18).

The consistency between the new data and previous results obtained using the EPM method suggest that controls on the zeta potential on the crude oil interface are similar, irrespective of whether the oil comprises droplets in an emulsion, or a wetting layer or film on a solid surface.

5.3. Implications for the behaviour of crude oil in industrial and natural processes

The zeta potential of the crude oil interface plays an important role in controlling the stability of oil-in-water emulsions (e.g. [45,93,96]), the wetting behaviour of crude oil on solid surfaces in the presence of aqueous electrolytes (e.g. [17,18,44,51]), and on the electrokinetic response of crude oil (e.g. [56]). The data reported here allow the impact of electrolyte composition on crude oil zeta potential to be estimated, although there are still significant gaps in data and understanding. The range of electrolyte compositions and experimental conditions remains limited and needs to be substantially expanded to cover a wider variety of industrial and natural systems. Data exploring the impact of divalent ions beyond Ca^{2+} and Mg^{2+}, complex electrolytes containing a mixture of ionic species, and conditions of elevated temperature, are still required. A key remaining uncertainty concerns the effect of crude oil composition, and the relationship between bulk and interfacial oil properties.

The wetting behaviour of crude oil is of particular importance in remediation of contaminated soils and rocks, and in oil production from subsurface reservoirs. One approach to recover this oil is to inject water into the contaminated rock or reservoir, which displaces the oil towards production boreholes. Numerous studies have suggested that the efficiency with which the oil is recovered is impacted by the composition of the injected water (see Jackson et al. [51] and [9] for reviews). It has been suggested that oil recovery is higher if the injected water modifies

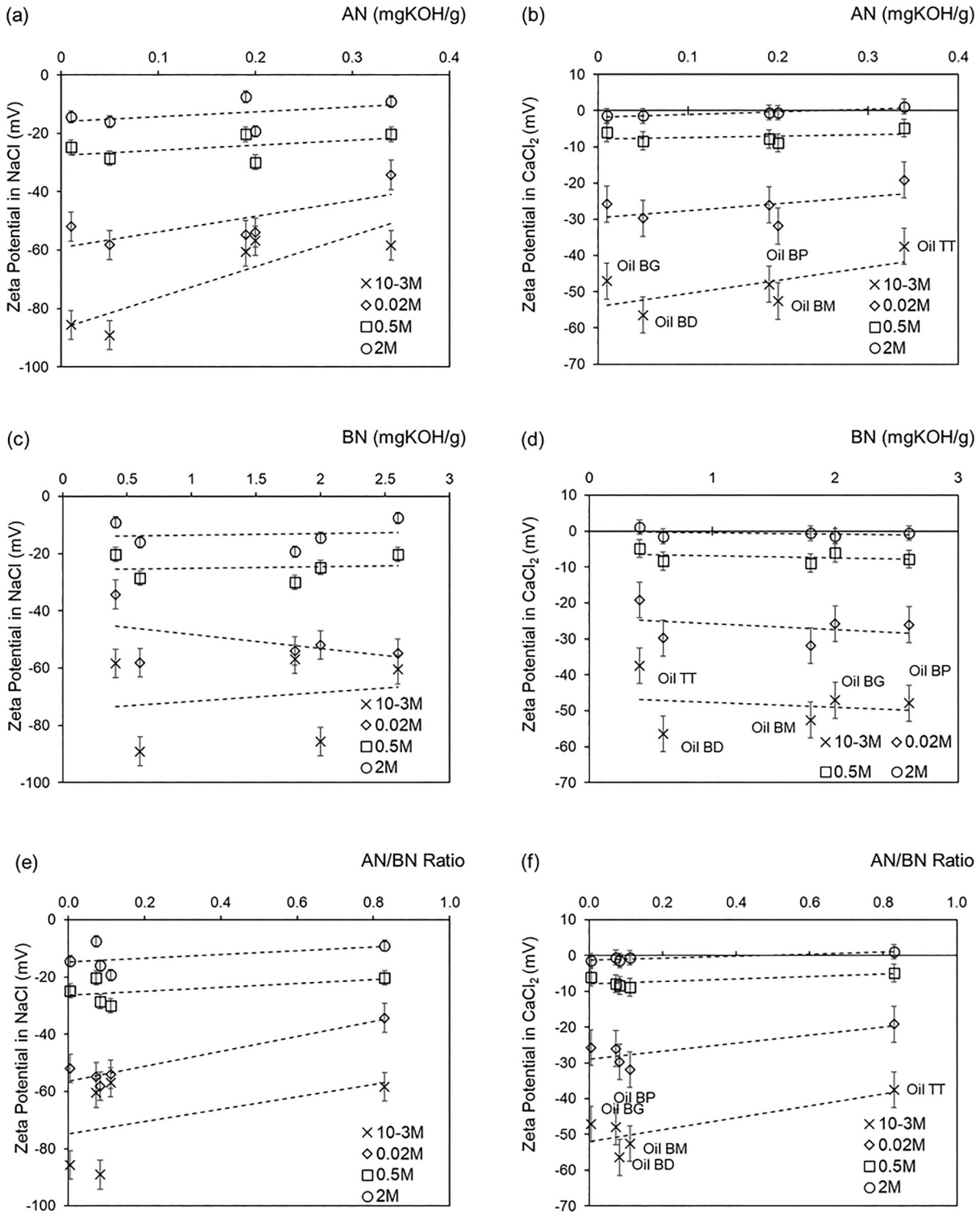

Fig. 17. Zeta potential data obtained using NaCl (plots a, c, e) and CaCl2 (plots b, d, f) electrolytes of varying ionic strengths plotted against (a, b) the AN of the oil, (c, d) the BN of the oil and (e, f) the AN/BN ratio of the oil. Dashed lines denote linear fit to the data, chosen in the absence of a strong theoretical basis to support higher order regressions. Data extracted from Fig. 12.

the zeta potential at the mineral interface in such a way that it increases the electrostatic repulsion between the crude oil and mineral interfaces [24,49]. For example, if the crude oil interface is negatively charged, then the water composition should be chosen to make the zeta potential at the mineral interface more negative, and vice-versa. However, as we show here, the water composition will also modify the zeta potential on the crude-oil surface, so this must be accounted for when identifying the optimum composition for injection. Previous studies have neglected this important consideration, assuming the zeta potential of the oil maintains the same polarity, irrespective of the water composition. High concentrations of Ca^{2+} and/or low pH can yield positive zeta potential on the crude oil interface. Other divalent ions and combination of divalent ions on complex natural or engineered brines may also yield a positive crude oil zeta potential.

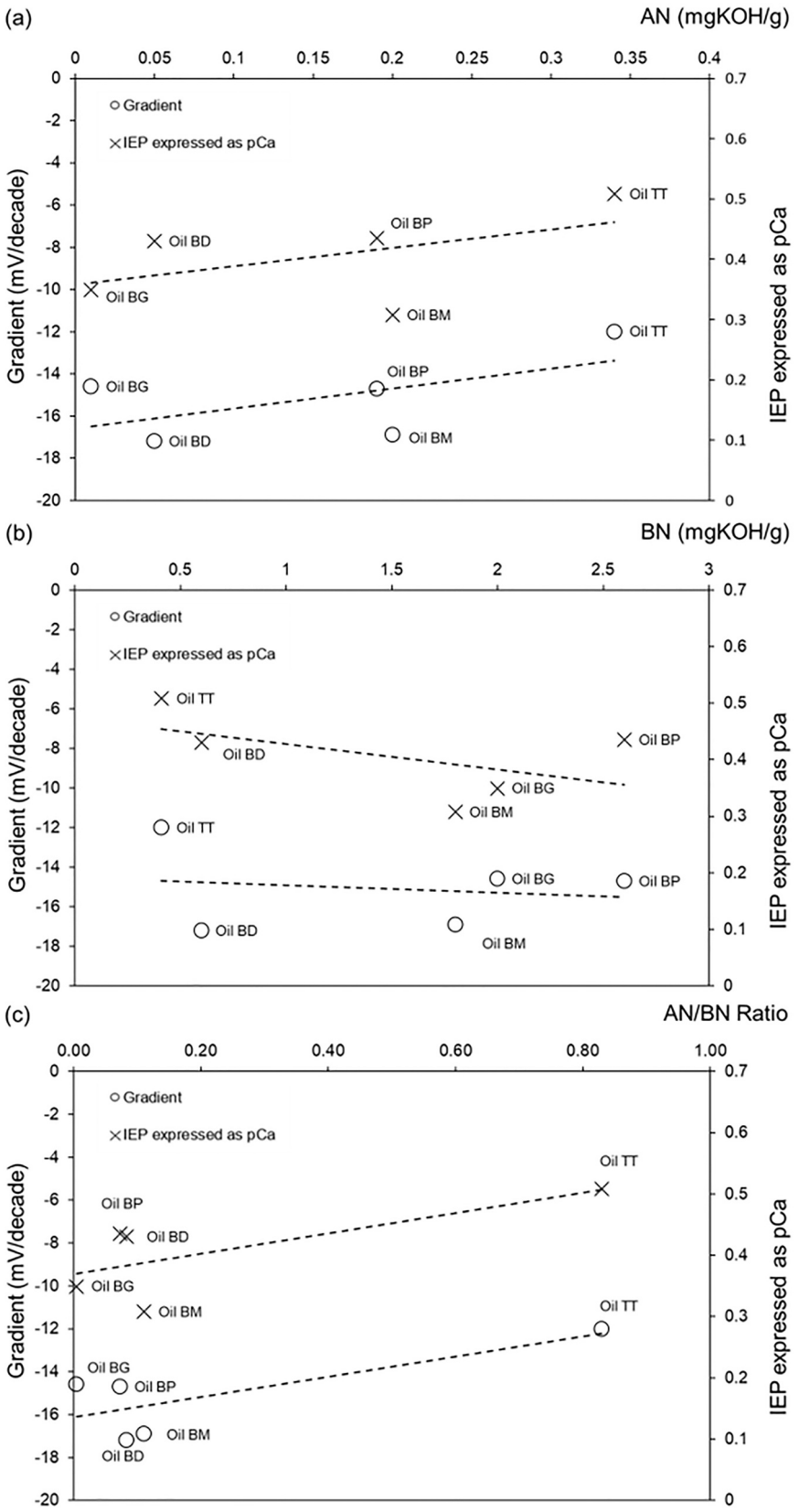

Fig. 18. The gradient of the trend line fitted to the data for each crude oil in Fig. 14, and the associated IEP expressed as pCa, plotted against the measured (a) AN, (b) BN and (c) AN/BN ratio of the crude oils. Dashed lines denote linear fit to the data, chosen in the absence of a strong theoretical basis to support higher order regressions.

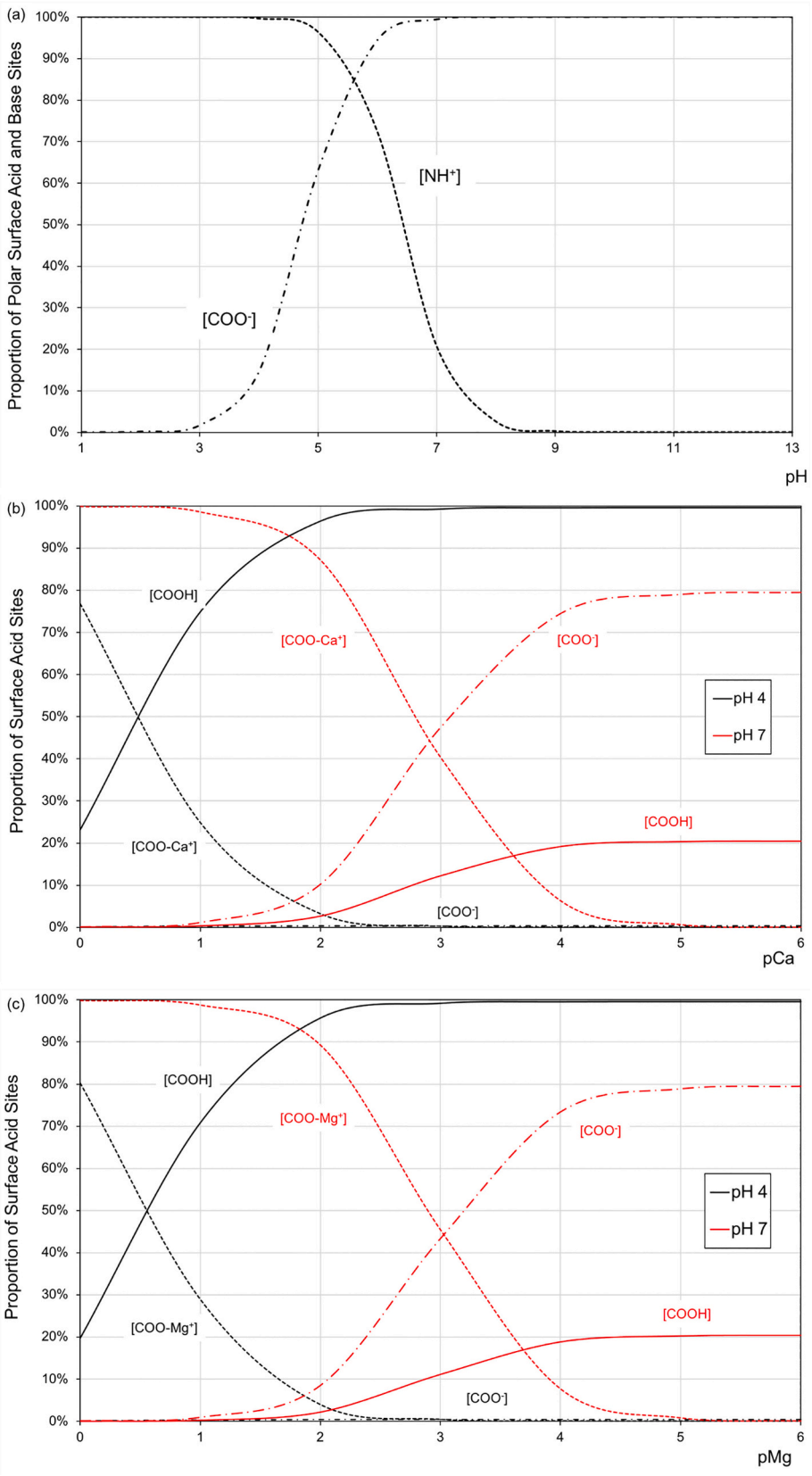

Fig. 19. Surface complexation model of Bonto et al. [13] (Table 6) showing (a) the proportion of surface acid sites that are negatively charged, and base sites that are positively charged, as a function of pH, and (b) and (c) the proportion of surface acid sites that are positively charged, neutral or negatively charged as a function of (b) pCa and (c) pMg. In (b) and (c), solid lines represent neutral acid sites; dot-dashed lines represent negatively charged acid sites and dashed lines represent positively charged acid sites; black lines represent pH 4 and red lines pH 7. (For interpretation of the references to colour in this figure legend, the reader is referred to the web version of this article.)

Removal of crude oil from contaminated rocks and soils can be achieved by the application of electrical fields, in a process termed electrokinetic remediation (e.g. [56]). Remediation can be applied with a static electrolyte saturating the pore-space, in which case the only cause of ion transport is application of the electric field. Remediation can also be applied with an electrolyte flowing through the pore-space, in which case ion transport is caused by application of the electric field and flow of the electrolyte. Remediation has been observed to be more

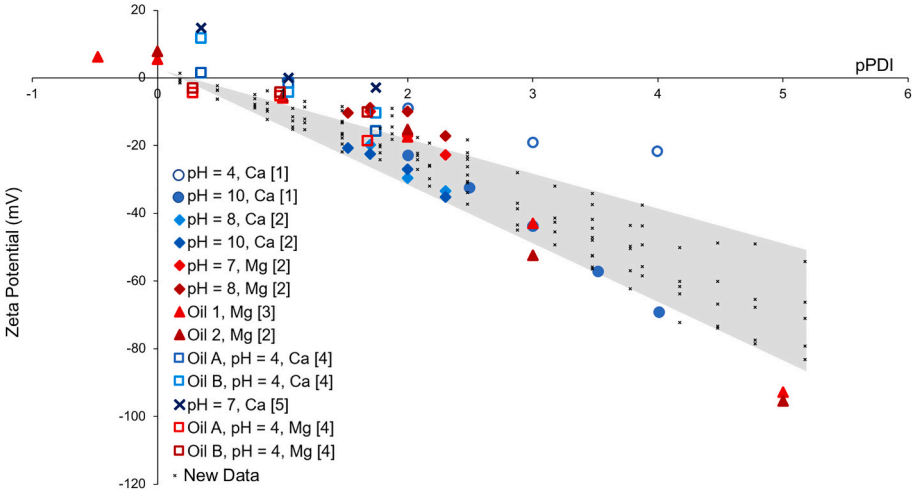

Fig. 20. Zeta potential data from Fig. 14 (small crosses) plotted with previously published data from Fig. 4. The gray shaded region represents the spread of the new data reported here. As in Fig. 4, data from [1] Chow et al. [21] [2] Takeya et al. [85] [3] Lu et al. [62] [4] Nasralla and Nasr-El-Din [68] [5] Pooryousefy et al. [74] [6] Takeya et al. [86].

effective in the flowing application. The flowing electrolyte can be chosen to have a different composition to the initial resident electrolyte. The crude oil zeta potential is an important parameter required for the design and modelling of such processes yet the parameter space available is currently limited to identify the optimum electrolyte composition to maximise the amount of crude oil that is remediated from contaminated zones.

6. Conclusions

- The zeta potential of crude oil emulsions in aqueous solution depends on pH, with higher pH yielding more negative zeta potential and lower pH yielding less negative, or positive, zeta potential. The experimentally-determined IEP in simple NaCl electrolytes lies in the pH range 3–5 for the range of crude oils reported. Close to the IEP, the zeta potential varies linearly with pH, consistent with simple Nernstian behaviour of the crude oil interface in aqueous solution. The sensitivity of the zeta potential to pH decreases with increasing ionic strength in simple NaCl electrolytes.
- The zeta potential of crude oil also depends on the concentration of divalent Ca^{2+} and Mg^{2+} ions, with higher pCa and/or pMg yielding more negative zeta potential and lower pCa and/or pMg yielding less negative zeta potential. Positive zeta potential at low pCa and pMg (expressed generally as pPDI) has been observed for some crude oils, and the experimentally-determined IEP expressed as pPDI lies in the range 0–1 for the range of crude oils reported. Close to the IEP, expressed as pPDI, the zeta potential varies linearly with pPDI, again consistent with Nernstian behaviour of the crude oil interface in aqueous solution.
- The sensitivity of the zeta potential to pCa and pMg decreases with decreasing pH and/or increasing total ionic strength in simple $CaCl_2$ and $MgCl_2$ electrolytes. The sensitivity to pCa is higher than the sensitivity to pMg. The impact of other multivalent ions on the zeta potential of the crude oil surface has not been tested, although such ions are often present in natural brines and engineered electrolytes.
- Only a few studies have measured the zeta potential of crude oils in complex, high ionic strength electrolytes or at elevated temperature. Experimental data exploring the effect of temperature on the zeta potential of crude oil in aqueous solution are too sparse and contradictory to allow firm conclusions to be drawn.
- Compared to non-polar oils, crude oils return a far broader range of zeta potential for given values of pH, divalent ion concentration and total electrolyte ionic strength; they also show a broader sensitivity to variations in pH and divalent ion concentration. The variability across different crude oils is in marked contrast to the consistent behaviour observed for non-polar oils.
- New zeta potential data reported here suggest a weak relationship between zeta potential and the acid number of the crude oil for both NaCl and $CaCl_2$ electrolytes but published data show no clear or consistent relationships between zeta potential and bulk oil properties such as acid or base number (AN or BN).
- The development of electrical charge at the interface of non-polar oils and other hydrophobes in aqueous solution has been interpreted to represent preferential adsorption of the hydroxide ion and to depend only on the electrolyte properties. However, the data compiled here suggest that charge development on the crude oil surface also depends on properties of the crude oil, such as the presence of interfacially-active polar organic molecules such as asphaltenes and resins. The role of these polar molecules in controlling the development of surface charge remains a key question.
- The zeta potential of wetting crude oil layers in aqueous electrolytes shows consistent behaviour with that obtained on emulsions of the crude oil and can be measured using the streaming potential method (SPM) by preparing a strongly oil-wet porous substrate in which the solid surfaces are coated with crude oil. Data obtained using the SPM are comparable to that obtained using conventional electrophoretic potential methods on emulsions (EPM).

Declaration of Competing Interest

The authors declare no conflicts of interest.

Data availability

Data will be made available on request.

Acknowledgments

Collini was supported by the UK Engineering and Physical Sciences Research Council (EPSRC) and bp via an industrial CASE award.

References

[1] Abdel-Raouf ME-S. Crude oil emulsions – composition, stability and characterization. IntechOpen; 2012.

[2] Al-Khdheeawi EA, Vialle S, Barifcani A, Sarmadivaleh M, Iglauer S. Effect of wettability heterogeneity and reservoir temperature on CO_2 storage efficiency in deep saline aquifers. Int J Greenh Gas Control 2018;68:216–29.
[3] Al Mahrouqi D, Vinogradov J, Jackson MD. Zeta potential of artificial and natural calcite in aqueous solution. Adv Colloid Interface Sci 2017;240:60–76.
[4] Alroudhan A, Vinogradov J, Jackson MD. Zeta potential of intact natural limestone: impact of potential-determining ions Ca, Mg and SO4. Colloids Surf A Physicochem Eng Asp 2016;493:83–98.
[5] Alshakhs MJ, Kovscek AR. Understanding the role of electrolyte ionic composition on oil recovery by assessment of wettability from colloidal forces. Adv Colloid Interface Sci 2016;233:126–38.
[6] Amott E. Observations relating to the wettability of porous rock. Trans AIME 1959; 216:156–62.
[7] Andersen SI, Chandra MS, Chen J, Zeng BY, Zou F, Mapolelo M, et al. Detection and impact of carboxylic acids at the crude oil–water interface. Energy Fuel 2016;30: 4475–85.
[8] Anderson WG. Wettability literature survey-part 1: rock/oil/electrolyte interactions and the effects of core handling on wettability. J Petrol Tech 1986;38: 1125–44.
[9] Bartels WB, Mahani H, Berg S, Hassanizadeh SM. Literature review of low salinity waterflooding from a length and timescale perspective. Fuel 2019;236:338–53.
[10] Beattie JK, Djerdjev AM. The pristine oil/water interface: surfactant-free hydroxide-charged emulsions. Angew Chem Int Ed 2004;116:3652–5.
[11] Beattie JK, Djerdjev AM, Franks GV, Warr GG. Dipolar anions are not preferentially attracted to the oil/water interface. J Phys Chem 2005;109:15675–6.
[12] Bertheussen A, Simon S, Sjöblom J. Equilibrium partitioning of naphthenic acids and bases and their consequences on interfacial properties. Colloids Surf A Physicochem Eng Asp 2017;529:45–56.
[13] Bonto M, Eftekhari AA, Nick HM. An overview of the oil-electrolyte interfacial behavior and a new surface complexation model. Sci Rep 2019;9:6072.
[14] Brady PV, Krumhansl JL. A surface complexation model of oil–brine–sandstone interfaces at 100°C: low salinity waterflooding. J Petrol Sci Eng 2012;81:171–6.
[15] Brady PV, Morrow NR, Fogden A, Deniz V, Loahardjo N, Winoto W. Electrostatics and the low salinity effect in sandstone reservoirs. Energy Fuel 2015;29:666–77.
[16] Buckley JS, Liu Y, Xie X, Morrow NR. Asphaltenes and crude oil wetting - the effect of oil composition. SPE J 1997;2:107–19.
[17] Buckley JS, Liu Y. Some mechanisms of crude oil/electrolyte/solid interactions. J Petrol Sci Eng 1998;20:155–60.
[18] Buckley JS, Takamura K, Morrow NR. Influence of electrical surface charges on the wetting properties of crude oils. SPE Reserv Eng 1989;4:332–40.
[19] Chaverot P, Cagna A, Glita S, Rondelez F. Interfacial tension of bitumen– water interfaces. Part 1: influence of endogenous surfactants at acidic pH. Energy Fuel 2008;22:790–8.
[20] Chow RS, Takamura K. The electric properties of the bitumen/water interface part II. Application of the ionizable surface-group model. Colloids Surf 1985;15:35–48.
[21] Chow RS, Takamura K. Electrophoretic mobilities of bitumen and conventional crude-in-water emulsions using the laser doppler apparatus in the presence of multivalent cations. J Colloid Interface Sci 1988;125:212–25.
[22] Chvedov D, Ostap S, Le T. Surface properties of red mud particles from potentiometric titration. Colloids Surf A Physicochem Eng Asp 2001;182:131–41.
[23] Collini H, Jackson MD. Relationship between zeta potential and wettability in porous media: insights from a simple bundle of capillary tubes model. J Colloid Interface Sci 2022;608:605–21.
[24] Collini H, Li S, Jackson MD, Agenet N, Rashid B, Couves J. Zeta potential in intact carbonates at reservoir conditions and its impact on oil recovery during controlled salinity waterflooding. Fuel 2020;266:116927.
[25] Creux P, Lachaise J, Graciaa A, Beattie JK, Djerdjev AM. Strong specific hydroxide ion binding at the pristine oil/water and air/water interfaces. J Phys Chem B 2009; 113:14146–50.
[26] Creux P, Lachaise J, Graciaa A, Beattie JK. Specific cation effects at the hydroxide-charged air/water interface. J Phys Chem C 2007;111:3753–5.
[27] Czarnecki J. Stabilization of water in crude oil emulsions. Part 2. Energy Fuel 2009; 23:1253–7.
[28] Das S, Thundat T, Mitra SK. Analytical model for zeta potential of asphaltene. Fuel 2013;108:543–9.
[29] Delgado ÁV, González-Caballero F, Hunter RJ, Koopal LK, Lyklema J. Measurement and interpretation of electrokinetic phenomena. J Colloid Interface Sci 2007;309:194–224.
[30] Dubey ST, Doe PH. Base number and wetting properties of crude oils. SPE Reserv Eng 1993;8:195–200.
[31] Dukhin A, Dukhin S, Goetz P. Electrokinetics at high ionic strength and hypothesis of the double layer with zero surface charge. Langmuir 2005;21:9990–7.
[32] Dunstan DE, Saville DA. Electrophoretic mobility of colloidal alkane particles in electrolyte solutions. J Chem Soc Faraday Trans 1992;88:2031–3.
[33] Farooq U, Simon S, Tweheyo MT, Sjöblom J, Øye G. Electrophoretic measurements of crude oil fractions dispersed in aqueous solutions of different ionic compositions—evaluation of the interfacial charging mechanisms. J Dispers Sci Technol 2013;34:1376–81.
[34] Foxall T, Peterson GC, Rendall HM, Smith AL. Charge determination at the calcium salt/aqueous solution interface. J Chem Soc Faraday Trans 1979;75:1034–9.
[35] Franks GV, Djerdjev AM, Beattie JK. Absence of specific cation or anion effects at low salt concentrations on the charge at the oil/water interface. Langmuir 2005;21: 8670–4.
[36] Gan W, Wu W, Yang F, Hu D, Fang H, Lan Z, et al. The behavior of hydroxide and hydronium ions at the hexadecane–water interface studied with second harmonic generation and zeta potential measurements. Soft Matter 2017;13:7962–8.
[37] Glover PWJ, Walker E, Jackson MD. Streaming-potential coefficient of reservoir rock: a theoretical model. Geophysics 2012;77:D17–43.
[38] Gopmanadal PP, Bhattacharyya S, Ohshima H. On the similarity between the electrophoresis of a liquid drop and a spherical hydrophobic particle. Colloid Polym Sci 2017;295:2077–82.
[39] Gopmandal PP, Duval JFL. Electrostatics and electrophoresis of engineered nanoparticles and particulate environmental contaminants: beyond zeta potential-based formulation. Curr Opin Colloid Interface Sci 2022;60:101605.
[40] Grate JW, Warner MG, Pittman JW, Dehoff KJ, Wietsma TW, Zhang C, et al. Silane modification of glass and silica surfaces to obtain equally oil-wet surfaces in glass-covered silicon micromodel applications. Water Resour Res 2013;49:4724–9.
[41] Gray-Weale A, Beattie JK. An explanation for the charge on water's surface. Phys Chem Chem Phys 2009;11:10994–1005.
[42] Guo J, Liu Q, Li M, Wu Z, Christy AA. The effect of alkali on crude oil/water interfacial properties and the stability of crude oil emulsions. Colloids Surf A Physicochem Eng Asp 2006;2006(273):213–8.
[43] Havre TE, Sjöblom J, Vindstad JE. Oil/water-partitioning and interfacial behavior of naphthenic acids. J Dispers Sci Technol 2003;24:789–801.
[44] Hirasaki G. Wettability: fundamentals and surface forces. SPE Form Eval 1991;6: 217–26.
[45] Hunter RJ. Measuring zeta potential in concentrated industrial slurries. Colloids Surf A Physicochem Eng Asp 2001;195:205–14.
[46] Hunter RJ. Zeta potential in colloid science: principles and applications. Academic Press; 2013.
[47] Hutin A, Argillier JF, Langevin D. Mass transfer between crude oil and water. Part 1: effect of oil components. Energy Fuel 2014;28:7331–6.
[48] Hutin A, Argillier JF, Langevin D. Mass transfer between crude oil and water. Part 2: effect of sodium dodecyl benzenesulfonate for enhanced oil recovery. Energy Fuel 2014;28:7337–42.
[49] Jackson MD, Al-Mahrouqi D, Vinogradov J. Zeta potential in oil-water-carbonate systems and its impact on oil recovery during controlled salinity water-flooding. Sci Rep 2016;6:37363.
[50] Jackson MD, Vinogradov J. Impact of wettability on laboratory measurements of streaming potential in carbonates. Colloids Surf A Physicochem Eng Asp 2012;393: 86–95.
[51] Jackson MD, Vinogradov J, Hamon G, Chamerois M. Evidence, mechanisms and improved understanding of controlled salinity waterflooding part 1: sandstones. Fuel 2016;185:772–93.
[52] Khair AS, Squires TM. The influence of hydrodynamic slip on the electrophoretic mobility of a spherical colloidal particle. Phys Fluids 2009;21:042001.
[53] Kobayash M. An analysis on electrophoretic mobility of hydrophobic polystyrene particles with low surface charge density: effect of hydrodynamic slip. Colloid Polym Sci 2020;298:1313–8.
[54] Kokal S, Tang T, Schramm L, Sayegh S. Electrokinetic and adsorption properties of asphaltenes. Colloids Surf A Physicochem Eng Asp 1995;94:253–65.
[55] Kolltveit Y. Relationship between crude oil composition and physical-chemical properties. MSc Thesis. The University of Bergen; 2016.
[56] Korolev VA, Romanyukha OV, Abyzova AM. Electrokinetic remediation of oil-contaminated soils. J Environ Sci Health A 2008;43:876–80.
[57] Krevor S, Blunt MJ, Benson SM, Pentland CH, Reynolds C, Al-Menhali A, et al. Capillary trapping for geologic carbon dioxide storage–from pore scale physics to field scale implications. Int J Greenh Gas Control 2015;40:221–37.
[58] Kumar S, Mahto V. Use of a novel surfactant to prepare oil-in-water emulsion of an Indian heavy crude oil for pipeline transportation. Energy Fuel 2017;31:12010–20.
[59] Kundu P, Kumar V, Mishra IM. Modeling the steady-shear rheological behavior of dilute to highly concentrated oil-in-water (o/w) emulsions: effect of temperature, oil volume fraction and anionic surfactant concentration. J Petrol Sci Eng 2015; 129:189–204.
[60] Li S, Leroy P, Heberling F, Devau N, Jougnot D, Chiaberge C. Influence of surface conductivity on the apparent zeta potential of calcite. J Colloid Interface Sci 2016; 468:262–75.
[61] Lin Q, Bijeljic B, Berg S, Pini R, Blunt MJ, Krevor S. Minimal surfaces in porous media: pore-scale imaging of multiphase flow in an altered-wettability Bentheimer sandstone. Phys Rev E 2019;99:063105.
[62] Lu Y, Najafabadi NF, Firoozabadi A. Effect of temperature on wettability of oil/electrolyte/rock systems. Energy Fuel 2017;31:4989–95.
[63] Mahani H, Keya AL, Berg S, Bartels W-B, Nasralla R, Rossen WR. Insights into the mechanism of wettability alteration by low-salinity flooding (LSF) in carbonates. Energy Fuel 2015;29:1352–67.
[64] Mahani H, Menezes R, Berg S, Fadili A, Nasralla R, Voskov D, et al. Insights into the impact of temperature on the wettability alteration by low salinity in carbonate rocks. Energy Fuel 2017;31:7839–53.
[65] Manciu M, Ruckenstein E. Ions near the air/water interface: I. Compatibility of zeta potential and surface tension experiments. Colloids Surf A Physicochem Eng Asp 2012;400:27–35.
[66] Marinova KG, Alargova RG, Denkov ND, Velev OD, Petsev DN, Ivanov IB, et al. Charging of oil-water interfaces due to spontaneous adsorption of hydroxyl ions. Langmuir 1996;12:2045–51.
[67] Mehraban MF, Ayatollahi S, Sharifi M. Role of divalent ions, temperature, and crude oil during water injection into dolomitic carbonate oil reservoirs. Oil Gas Sci Technol–Revue d'IFP Energies Nouvelles 2019;74:36.
[68] Nasralla RA, Nasr-El-Din HA. Impact of cation type and concentration in injected electrolyte on oil recovery in sandstone reservoirs. J Petrol Sci Eng 2014;122: 384–95.
[69] Nenningsland AL, Simon S, Sjoblom J. Surface properties of basic components extracted from petroleum crude oil. Energy Fuel 2010;24:6501–5.

[70] Nespolo SA, Bevan MA, Chan DYC, Grieser F, Stevens GW. Hydrodynamic and electrokinetic properties of decane droplets in aqueous sodium dodecyl sulfate solutions. Langmuir 2001;17:7210–8.
[71] Ohshima H. Electrophoresis of charged particles and drops. In: Interfacial electrokinetics and electrophoresis. 1st ed. CRC Press; 2002.
[72] Onaizi SA. Effect of oil/water ratio on rheological behavior, droplet size, zeta potential, long-term stability, and acid-induced demulsification of crude oil/water nanoemulsions. J Petrol Sci Eng 2022;209:109857.
[73] Parra-Barraza H, Hernandez-Montiel D, Lizardi J, Hernandez J, Herrera Urbina R, Valdez MA. The zeta potential and surface properties of asphaltenes obtained with different crude oil/*n*-heptane proportions. Fuel 2003;82:869–74.
[74] Pooryousefy E, Xie Q, Chen Y, Sari A, Saeedi A. Drivers of low salinity effect in sandstone reservoirs. J Mol Liq 2018;250:396–403.
[75] Revil A, Pezard PA, Glover PWJ. Streaming potential in porous media: 1. Theory of the zeta potential. J Geophys Res 1999;104:20021–31.
[76] Roger K, Cabane B. Why are hydrophobic/water interfaces negatively charged? Angew Chem Int Ed 2012;51:5625–8.
[77] Rønningsen HP, Sjöblom J, Mingyuan L. Water-in-crude oil emulsions from the Norwegian continental shelf: ageing of crude oils and its influence on the emulsion stability. Colloids Surf A Physicochem Eng Asp 1995;97:119–28.
[78] Seifert WK, Howells WG. Interfacially active acids in a California crude oil. Anal Chem 1969;41:554–62.
[79] Shi C, Zhang L, Xie L, Lu X, Liu Q, Mantilla CA, et al. Interaction mechanism of oil-in-water emulsions with asphaltenes determined using droplet probe AFM. Langmuir 2016;32:2302–10.
[80] Shi C, Xie L, Zhang L, Lu X, Zeng H. Probing the interaction mechanism between oil droplets with asphaltenes and solid surfaces using AFM. J Colloid Interface Sci 2020;558:173–81.
[81] Simanzhenkov V, Idem R. Crude oil chemistry. CRC Press; 2003.
[82] Stachurski J, Michalek M. The effect of the zeta potential on the stability of a non-polar oil-in-water emulsion. J Colloid Interface Sci 1996;184:433–6.
[83] Szymula M, Janusz W, Jabloriski J. Electrochemical properties of asphaltene particles in aqueous solutions. J Dispers Sci Technol 2000;21:785–802.
[84] Takamura K, Chow RS. The electric poperties of the bitumen/water interface part II: application of the ionizable surface-group model. Colloids Surf 1985;15:35–48.
[85] Takeya M, Shimokawara M, Elakneswaran Y, Nawa T, Takahashi S. Predicting the electrokinetic properties of the crude oil/electrolyte interface for enhanced oil recovery in low salinity water flooding. Fuel 2019;235:822–31.
[86] Takeya M, Shimokawara M, Elakneswaran Y, Okano H, Nawa T. Effect of acid number on the electrokinetic properties of crude oil during low salinity waterflooding. Energy Fuel 2019;33:4211–8.
[87] Tetteh JT, Alimoradi S, Brady PV, Ghahfarokhi RB. Electrokinetics at calcite-rich limestone surface: understanding the role of ions in modified salinity waterflooding. J Mol Liq 2020;297:111868.
[88] Uematsu Y, Bonthius DJ, Netz RR. Nanomolar surface-active charged impurities account for the zeta potential of hydrophobic surfaces. Langmuir 2020;36:3645–58.
[89] Vinogradov J, Jaafar MZ, Jackson MD. Measurement of streaming potential coupling coefficient in sandstones saturated with natural and artificial electrolytes at high salinity. J Geophys Res 2010;115:B12204.
[90] Vinogradov J, Jackson MD. Zeta potential in intact natural sandstones at elevated temperatures. Geophys Res Lett 2015;42:6287–94.
[91] Vinogradov J, Jackson MD, Chamerois M. Zeta potential in sandpacks: effect of temperature, electrolyte pH, ionic strength and divalent cations. Colloids Surf A Physicochem Eng Asp 2018;553:259–71.
[92] Walker E, Glover PWJ. Measurements of the relationship between microstructure, pH, and the streaming and zeta potentials of sandstones. Transp Porous Media 2017;121:183–206.
[93] Wiącek A, Chibowski E. Zeta potential, effective diameter and multimodal size distribution in oil/water emulsion. Colloids Surf A Physicochem Eng Asp 1999;159:253–61.
[94] Yang F, Tchoukov P, Dettman H, Teklebrhan RB, Liu L, Dabros T, et al. Asphaltene subfractions responsible for stabilizing water-in-crude oil emulsions. Part 2: molecular representations and molecular dynamics simulations. Energy Fuel 2015;29:4783–94.
[95] Yang F, Tchoukov P, Pensini E, Dabros T, Czarnecki J, Masliyah J, et al. Asphaltene subfractions responsible for stabilizing water-in-crude oil emulsions. Part 1: interfacial behaviors. Energy Fuel 2014;28:6897–904.
[96] Zhang J, Tian D, Lin M, Yang Z, Dong Z. Effect of resins, waxes and asphaltenes on water-oil interfacial properties and emulsion stability. Colloids Surf A Physicochem Eng Asp 2016;507:1–6.